Electronic Supplementary Material (ESI) for Catalysis Science & Technology.
This journal is © The Royal Society of Chemistry 2022

Supporting Information

For

Combining High Activity with Broad Monomer Scope: Indium Salan Catalysts in the Ring-Opening Polymerization of Various Cyclic Esters

Jonas Bruckmoser, Daniel Henschel, Sergei Vagin, Bernhard Rieger*

WACKER-Chair of Macromolecular Chemistry, Catalysis Research Center
Technical University of Munich
Lichtenbergstraße 4, 85748 Garching bei München, Germany.

*Corresponding Author; email: rieger@tum.de

Table of Contents

1. Experimental Section

Materials and Methods

All manipulations were carried out under argon atmosphere using standard Schlenk or glovebox techniques. Glassware was flame-dried under vacuum prior to use. Unless otherwise stated, all chemicals were purchased from Sigma-Aldrich, TCI Chemicals or ABCR and used as received. Solvents were obtained from an MBraun MB-SPS 800 solvent purification system and stored over 3 Å molecular sieves prior to use. β-BL was treated with BaO, dried over CaH_2 and distilled prior to use. ε-CL, ε-DL and γ-BL were distilled from CaH_2 prior to use. *rac*-LA was sublimed once prior to use. Deuterated chloroform ($CDCl_3$) and toluene (C_7D_8) were obtained from Sigma-Aldrich and dried over 3 Å molecular sieves. Proligand **L3** was prepared according to the literature.[1]

Nuclear magnetic resonance (NMR) spectra were recorded on a Bruker AV-III-500 spectrometer equipped with a QNP-Cryoprobe, AV-III-300 or AV-III-400 spectrometers at ambient temperature (298 K). ^{1}H and ^{13}C{^{1}H} NMR spectroscopic chemical shifts δ are reported in ppm relative to tetramethylsilane and were referenced internally to the relevant residual solvent resonances. The following abbreviations are used: br, broad; s, singlet; d, doublet; m, multiplet.
The tacticity of PHB was determined by integration of the carbonyl region of the ^{13}C{^{1}H} NMR spectrum whereas for PLA, the tacticity was calculated from the peak deconvoluted methine region of the ^{1}H{^{1}H} NMR spectrum.[2, 3]

Elemental analyses were measured with a EURO EA instrument from HEKAtech at the Laboratory for Microanalysis, Catalysis Research Center, Technical University of Munich.

Electrospray ionization mass spectrometry (ESI-MS) was measured with a Thermo Fisher Scientific Exactive Plus Orbitrap in the positive mode in acetonitrile.

Polymer weight-average molecular weight (M_w), number-average molecular weight (M_n) and polydispersity indices ($Đ = M_w/M_n$) were determined *via* gel permeation chromatography (GPC) relative to polystyrene standards on PL-SEC 50 Plus instruments from Polymer Laboratories. For PHB the analysis was performed at ambient temperatures using chloroform as the eluent at a flow rate of 1.0 mL min^{-1}. For PεCL, PεDL, PLA and PγBL the analysis was performed at

40°C using THF as the eluent at a flow rate of 1.0 mL min^{-1}. Molecular weights of PεCL and PLA were corrected with a Mark–Houwink factor of 0.56 and 0.58, respectively.[4]

General Polymerization Procedures

Typical polymerization of β-BL: In a glove box, initiator **2** (13.0 mg, 18.3 μmol) was dissolved in 1.55 mL of toluene and β-BL (300 μL, 315 mg, 3.66 mmol) was injected into the reaction, such that the overall concentration of β-BL was 2.0 M. After 15 min the polymerization was quenched by addition of 0.5 mL MeOH and conversion was determined by ^{1}H NMR spectroscopy of an aliquot. The mixture was precipitated into excess diethyl ether/pentane (1:1), filtered, washed with additional diethyl ether/pentane and dried under vacuum.

Typical immortal ROP of β-BL: In a glove box, initiator **2** was dissolved in toluene and the respective amount of a BnOH stock solution in toluene (0.080 M) was added. After 15 min of stirring, β-BL was injected into the reaction, such that the overall concentration of β-BL was 2.0 M. The rest of the procedure followed the general polymerization procedure.

Kinetic experiments of β-BL polymerization: In a glove box, the respective amount of initiator **2**, toluene and β-BL were mixed, such that the overall concentration of β-BL was 2.0 M. After certain time intervals, aliquots were taken from the reaction mixture, quenched with 0.4 mL hydrous $CDCl_3$ and conversion determined by ^{1}H NMR spectroscopy. The crude products were additionally analyzed by GPC.

Polymerization of β-BL with PO-activated **1**: In a glove box, initiator **1** (10.0 mg, 14.9 μmol) was dissolved in 1.24 mL of propylene oxide (PO) and the mixture stirred for 24 h at room temperature. After this preactivation time, β-BL (244 μL, 256 mg, 2.97 mmol) was injected into the reaction, such that the overall concentration of β-BL was 2.0 M. After certain time intervals, aliquots were taken from the reaction mixture, quenched with 0.4 mL hydrous $CDCl_3$ and conversion determined by ^{1}H NMR spectroscopy. The polymerization was quenched by addition of 0.5 mL MeOH, precipitated into excess diethyl ether/pentane (1:1), filtered, washed with additional diethyl ether/pentane and dried under vacuum. The isolated polymer and crude products were analyzed by GPC.

Typical polymerization of ε-CL: In a glove box, initiator **2** (4.0 mg, 5.6 μmol) was dissolved in 1.09 mL of toluene and ε-CL (312 μL, 321 mg, 2.81 mmol) was rapidly injected into the reaction, such that the overall concentration of ε-CL was 2.0 M. After 20 s the polymerization was quenched by rapid addition of 1.0 mL hydrous $CDCl_3$ and conversion was determined by

^{1}H NMR spectroscopy of an aliquot. The mixture was precipitated into excess methanol, filtered, washed with additional methanol and dried under vacuum.

Typical polymerization of ε-DL: In a glove box, initiator **2** (5.0 mg, 7.0 μmol) was dissolved in 0.46 mL of toluene and ε-DL (245 μL, 240 mg, 1.41 mmol) was injected into the reaction, such that the overall concentration of ε-DL was 2.0 M. After 2 h the polymerization was quenched by addition of 0.2 mL MeOH and conversion was determined by ^{1}H NMR spectroscopy of an aliquot. The mixture was precipitated into excess methanol, filtered, washed with additional methanol and dried under vacuum.

Typical polymerization of γ-BL: In a glove box, γ-BL (107 μL, 121 mg, 1.41 mmol) was added to initiator **2** (5.0 mg, 7.0 μmol) and the reaction mixture cooled to -35°C. After 24 h at -35°C the polymerization was quenched by addition of a cold solution of 1.0 mL benzoic acid in $CHCl_3$ (10 mg mL^{-1}) and conversion was determined by ^{1}H NMR spectroscopy of an aliquot. The mixture was precipitated into excess cold methanol, filtered and dried under vacuum.

Typical polymerization of purified *rac*-LA: In a glove box, sublimed *rac*-LA (406 mg, 2.81 mmol) was added to initiator **2** (4.0 mg, 5.6 μmol). The vial was sealed, removed from the glove box and placed in a preheated aluminum block at 130°C. After 10 min the polymerization was quenched by addition of 0.2 mL MeOH and conversion was determined by ^{1}H NMR spectroscopy of an aliquot. The mixture was dissolved in a minimal amount of dichloromethane and precipitated into excess pentane, filtered, washed with additional pentane and dried under vacuum.

Polymerization of unpurified *rac*-LA: The polymerization procedure was as described above but commercial grade *rac*-LA (99%, Sigma-Aldrich) was used as received instead of sublimed *rac*-LA.

Polymerization of unpurified *L*-LA: The polymerization procedure was as described above but commercial grade *L*-LA (98%, Sigma-Aldrich) was used as received instead of sublimed *rac*-LA.

Synthesis of Compounds

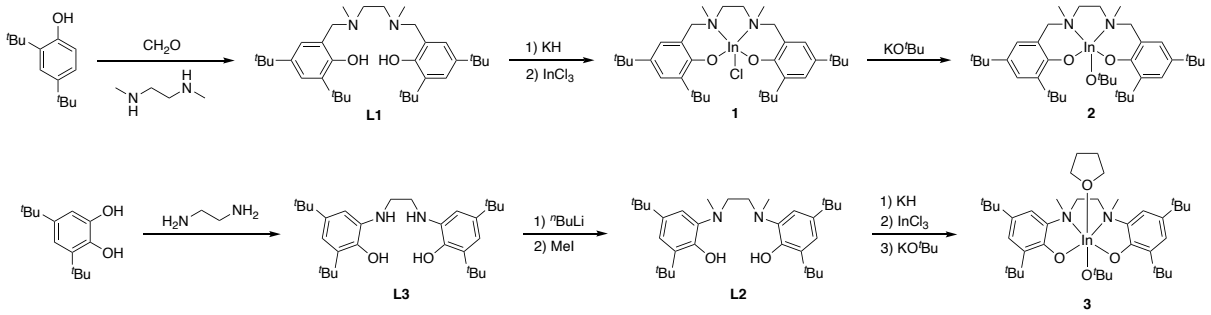

Scheme S1. Synthesis of indium complexes **1** – **3**. Complex **2** can also be prepared in a one-pot route starting from ligand **L1** (not shown).

Synthesis of Salan Ligand L1.

The synthesis followed a reported literature procedure.[5] 2,4-di-*tert*-butylphenol (8.25 g, 40.0 mmol) was dissolved in 20 mL of methanol and 15 mL aqueous formaldehyde solution (37 wt.%) and *N,N'*-dimethylethylenediamine (2.15 mL, 1.76 g, 20.0 mmol) were added. The reaction mixture was refluxed for 16 h. After cooling to room temperature, the colorless precipitate was filtered off, washed with 30 mL of methanol and dried *in vacuo* to give 9.09 g (87%) of **L1**.

^{1}H NMR (400 MHz, $CDCl_3$): δ 10.68 (br s, 2H, OH), 7.20 (d, J = 2.4 Hz, 2H, Ar-H), 6.80 (d, J = 2.4 Hz, 2H, Ar-H), 3.66 (s, 4H, Ar-CH_2), 2.63 (s, 4H, N-CH_2), 2.26 (s, 6H, N-Me), 1.40 (s, 18H, ^{t}Bu), 1.27 (s, 18H, ^{t}Bu). ^{13}C{^{1}H} NMR (101 MHz, $CDCl_3$): δ 154.3, 140.7, 135.8, 123.5, 123.1, 121.1, 62.9, 53.9, 41.8, 35.0, 34.3, 31.9, 29.8.

Synthesis of Catam Ligand L2.

The synthesis followed a reported literature procedure.[6] A solution of **L3** (1.87 g, 4.0 mmol) in 25 mL of THF was cooled to -78°C and *n*-butyllithium (2.5 M in hexane, 3.20 mL, 0.51 g, 8.0 mmol) was added dropwise. After stirring at -78°C for 15 min, the reaction mixture was allowed to warm to room temperature and stirred for an additional 2 h. Subsequently, methyl iodide (0.50 mL, 1.14 g, 8.0 mmol) was added, the solution stirred for 16 h at room temperature and then refluxed for an additional 5 h. The solvent was removed under reduced pressure, water (25 mL) added and the mixture extracted with dichloromethane (3×20 mL). The combined organic phases were washed with brine (20 mL), dried over $MgSO_4$ and the solvent removed under reduced pressure. The residue was recrystallized from methanol/dichloromethane (2:1) to give an off-white solid (1.37 g, 69%).

^{1}H NMR (400 MHz, $CDCl_3$): δ 8.37 (br s, 2H, OH), 7.13 (d, *J* = 2.4 Hz, 2H, Ar-H), 7.07 (d, *J* = 2.4 Hz, 2H, Ar-H), 2.87 (s, 4H, N-CH_2), 2.73 (s, 6H, N-Me), 1.42 (s, 18H, ^{t}Bu), 1.30 (s, 18H, ^{t}Bu). ^{13}C{^{1}H} NMR (101 MHz, $CDCl_3$): δ 148.6, 141.1, 138.6, 135.1, 120.7, 115.6, 57.1, 43.1, 35.2, 34.7, 31.9, 29.7.

Synthesis of Indium Complexes 1 – 3

Compound 1. The synthesis followed a reported literature procedure.[7] To a suspension of KH (0.24 g, 6.0 mmol) in 10 mL of THF, a solution of **L1** (1.57 g, 3.0 mmol) in 10 mL of THF was added dropwise. The resulting solution was stirred for 20 h at room temperature and then cooled to -78°C. A solution of $InCl_3$ (0.66 g, 3.0 mmol) in 10 mL of THF was added dropwise and after complete addition the reaction mixture was allowed to slowly warm to room temperature within 2 h and was then stirred for one additional hour. The reaction mixture was evaporated to dryness, the residue resuspended in 20 mL of dichloromethane, filtered over Celite and the solvent removed *in vacuo*. After washing with 5 mL of pentane, a colorless solid was obtained (1.45 g, 72%).
^{1}H NMR (400 MHz, $CDCl_3$): δ 7.30 (d, *J* = 2.5 Hz, 2H, Ar-H), 6.79 (d, *J* = 2.5 Hz, 2H, Ar-H), 4.84 (d, *J* = 12.0 Hz, 2H, Ar-CH_2), 3.28 – 3.17 (m, 4H, Ar-CH_2 and N-CH_2), 2.99 – 2.89 (m, 2H, N-CH_2), 2.42 (s, 6H, N-Me), 1.50 (s, 18H, ^{t}Bu), 1.27 (s, 18H, ^{t}Bu). ^{13}C{^{1}H} NMR (101 MHz, $CDCl_3$): δ 160.5, 139.9, 138.2, 125.3, 125.1, 119.9, 64.2, 55.6, 44.0, 35.4, 34.2, 31.9, 30.0. Anal. Calc. for $C_{34}H_{54}N_2O_2ClIn$: C, 60.67; H, 8.09; N, 4.16. Found: C, 61.21; H, 8.32; N, 4.16%.

Characterization data for compound **1** after being stored under air at room temperature for 3 months: ^{1}H NMR data as stated above; no decomposition was observed (Figure S7, S8). Anal. Calc. for $C_{34}H_{54}N_2O_2ClIn$: C, 60.67; H, 8.09; N, 4.16. Found: C, 61.41; H, 8.30; N, 4.17%.
Hydrolytic stability tests of compound **1** in solution: ca. 10 mg of **1** were dissolved in 0.5 ml hydrous $CDCl_3$ (water content: 110 ppm) and ^{1}H NMR spectra of the sample measured in regular intervals. Signals corresponding to free salan ligand **L1** were increasing steadily and after 20 h at room temperature 31% of **1** was decomposed (Figure S9).

Compound 2. KO^{t}Bu (67 mg, 0.6 mmol) was added to a solution of **1** (404 mg, 0.6 mmol) in 10 mL of THF. The resulting suspension was stirred for 16 h at room temperature, subsequently

filtered using a 0.45 μm PTFE syringe filter and the solvent removed *in vacuo*. The residue was washed with pentane (2×2 mL) to give a colorless solid (315 mg, 74%). Single crystals of **2** suitable for X-ray diffraction measurements were obtained by slow evaporation from a saturated toluene solution at room temperature.

^{1}H NMR (400 MHz, $CDCl_3$): δ 7.27 (d, J = 2.6 Hz, 2H, Ar-H), 6.74 (d, J = 2.6 Hz, 2H, Ar-H), 4.49 (d, J = 12.1 Hz, 2H, Ar-CH_2), 3.24 (d, J = 12.3 Hz, 2H, Ar-CH_2), 3.06 – 2.97 (m, 2H, N-CH_2), 2.90 – 2.81 (m, 2H, N-CH_2), 2.51 (s, 6H, N-Me), 1.45 (s, 18H, Ar-^{t}Bu), 1.27 (s, 18H, Ar-^{t}Bu), 1.24 (s, 9H, O-^{t}Bu). ^{13}C{^{1}H} NMR (101 MHz, $CDCl_3$): δ 161.6, 139.1, 136.8, 125.3, 124.6, 119.4, 63.8, 55.1, 44.0, 35.5, 35.4, 34.1, 31.9, 31.9, 30.2. Anal. Calc. for $C_{38}H_{63}N_2O_3In$: C, 64.22; H, 8.93; N, 3.94. Found: C, 64.33; H, 9.06; N, 3.82%.

Compound 2 – One-Pot-Route. To a suspension of KH (160 mg, 4.0 mmol) in 7 mL of THF, a solution of **L1** (1050 mg, 2.0 mmol) in 8 mL of THF was added dropwise. The resulting solution was stirred for 17 h at room temperature and then cooled to -78°C. A solution of $InCl_3$ (442 mg, 2.0 mmol) in 10 mL of THF was added dropwise and after complete addition the reaction mixture was allowed to slowly warm to room temperature within 2 h and was then stirred for an additional 2 h. Subsequently, KO^{t}Bu (224 mg, 2.0 mmol) was added to the reaction mixture and stirring continued for 23 h at room temperature. After filtration using a 0.45 μm PTFE syringe filter, removal of volatiles *in vacuo* and washing the residue with pentane (2×5 mL) a colorless solid was obtained (909 mg, 64%).

^{1}H and ^{13}C{^{1}H} NMR data as stated above. Anal. Calc. for $C_{38}H_{63}N_2O_3In$: C, 64.22; H, 8.93; N, 3.94. Found: C, 63.99; H, 9.04; N, 3.96%.

Compound 3. To a suspension of KH (64 mg, 1.6 mmol) in 3 mL of THF, a solution of **L2** (397 mg, 0.8 mmol) in 4 mL of THF was added dropwise. The resulting solution was stirred for 16 h at room temperature and then cooled to -78°C. A solution of $InCl_3$ (177 mg, 0.8 mmol) in 5 mL of THF was added dropwise and after complete addition the reaction mixture was allowed to slowly warm to room temperature within 2 h and was then stirred for an additional 2 h. Subsequently, KO^{t}Bu (90 mg, 0.8 mmol) was added to the reaction mixture and stirring continued for 21 h at room temperature. The cloudy solution was filtered using a 0.45 μm PTFE syringe filter and the solvent removed *in vacuo*. Recrystallization from pentane and additional washing with a minimal amount of cold pentane gave **3** as a colorless solid (193 mg, 32%). Multiple attempts for the isolation of single crystals of **3** suitable for X-ray diffraction measurements were unsuccessful.

^{1}H NMR (400 MHz, C_7D_8): δ 7.42 (d, *J* = 2.5 Hz, 2H, Ar-H), 6.94 (d, *J* = 2.5 Hz, 2H, Ar-H), 3.93 – 3.83 (m, 4H, THF), 2.71 (s, 6H, N-Me), 2.48 (d, *J* = 10.1 Hz, 2H, N-CH_2), 2.00 (d, *J* = 10.1 Hz, 2H, N-CH_2), 1.77 (s, 18H, Ar-^{t}Bu), 1.46 (s, 9H, O-^{t}Bu), 1.34 (s, 18H, Ar-^{t}Bu), 1.30 – 1.26 (m, 4H, THF). ^{13}C{^{1}H} NMR (101 MHz, C_7D_8): δ 157.7, 138.2, 136.1, 134.8, 122.3, 114.5, 69.8, 69.0, 58.3, 46.2, 35.9, 35.4, 34.5, 32.0, 30.0, 25.3. Anal. Calc. for $C_{40}H_{67}N_2O_4In$: C, 63.65; H, 8.95; N, 3.71. Found: C, 63.49; H, 9.16; N, 3.72%.

NMR Spectra of Compounds

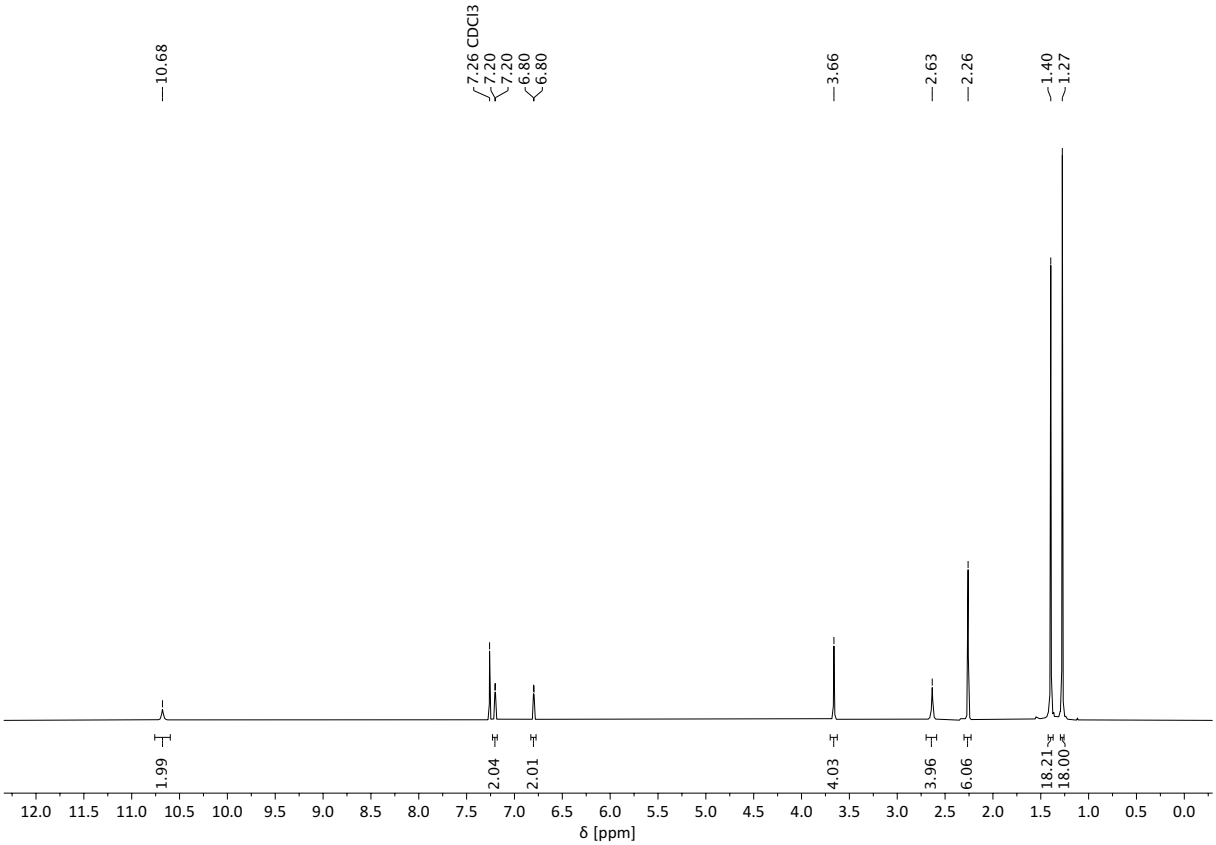

Figure S1. ^{1}H NMR spectrum ($CDCl_3$) of salan ligand **L1**.

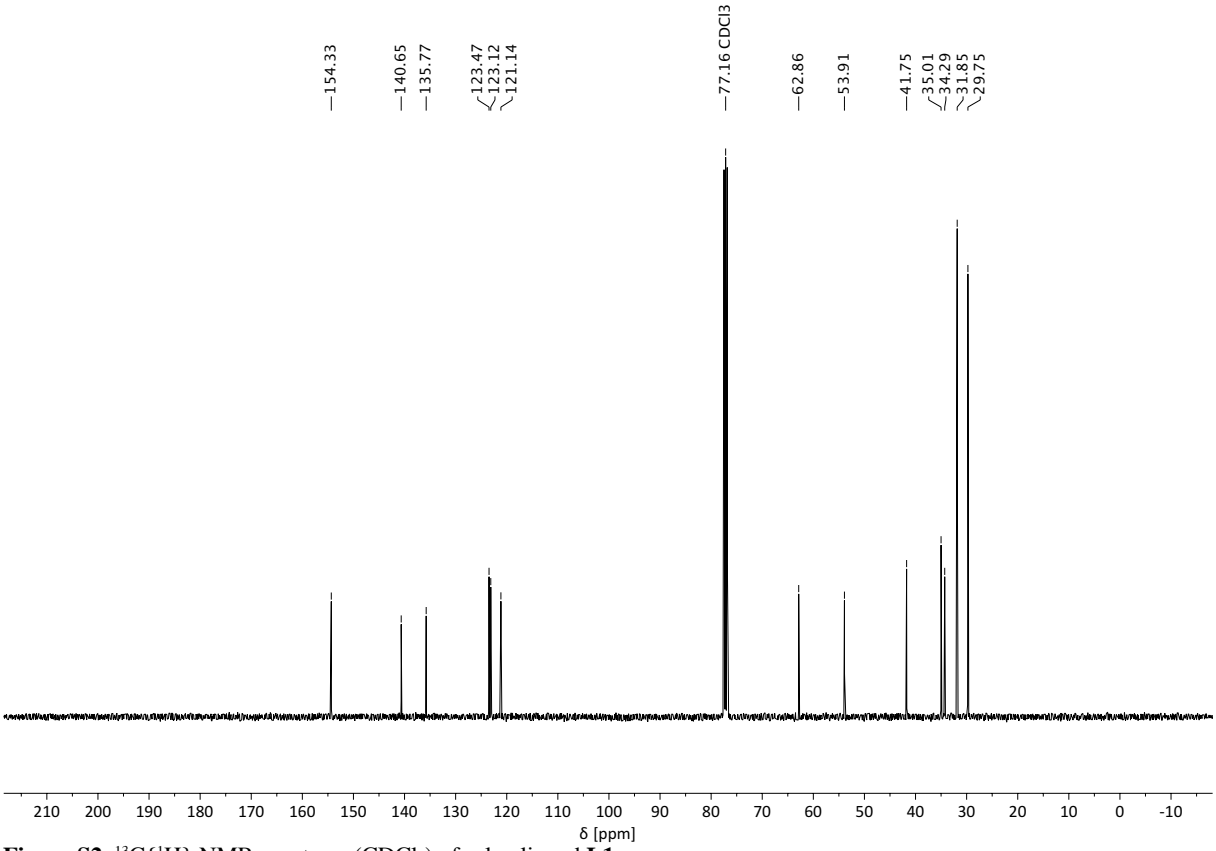

Figure S2. ^{13}C{^{1}H} NMR spectrum ($CDCl_3$) of salan ligand **L1**.

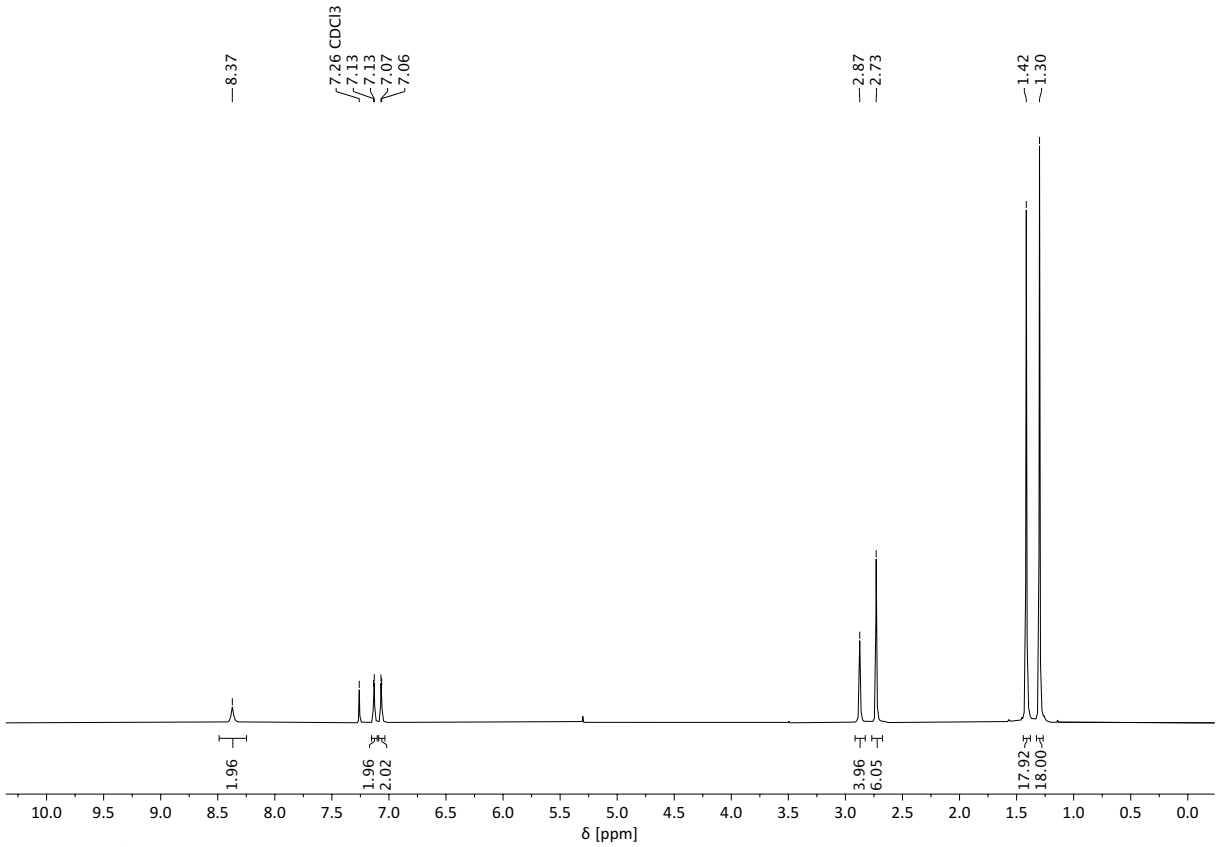

Figure S3. ^{1}H NMR spectrum ($CDCl_3$) of catam ligand **L2**.

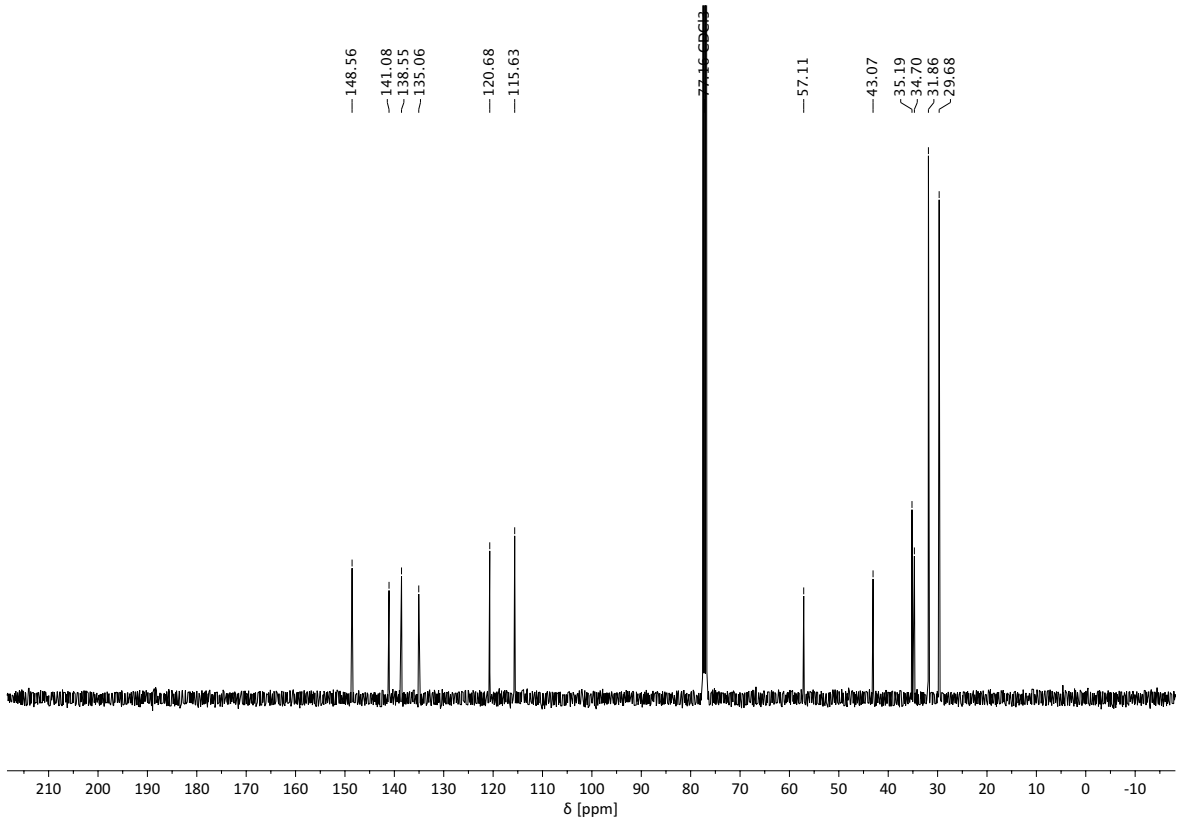

Figure S4. ^{13}C{^{1}H} NMR spectrum ($CDCl_3$) of catam ligand **L2**.

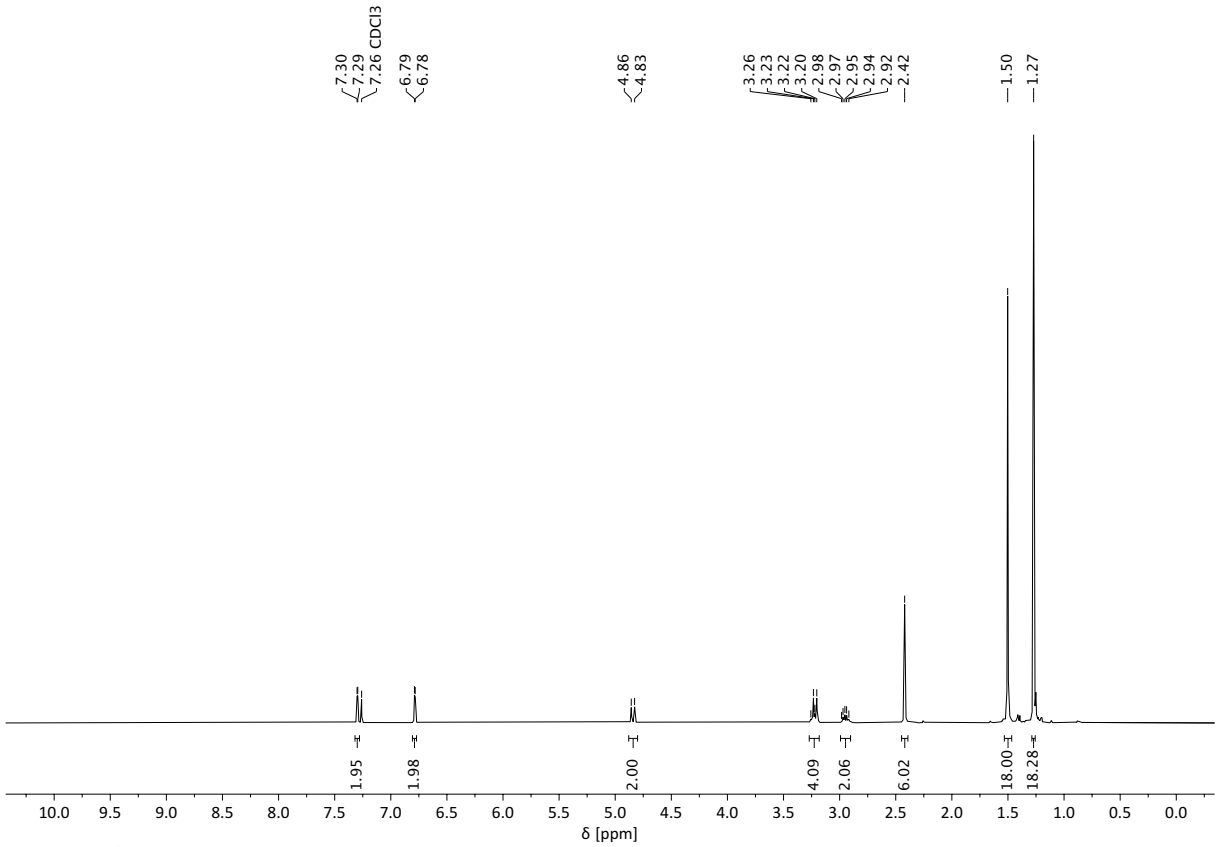

Figure S5. ^{1}H NMR spectrum ($CDCl_3$) of indium complex **1**.

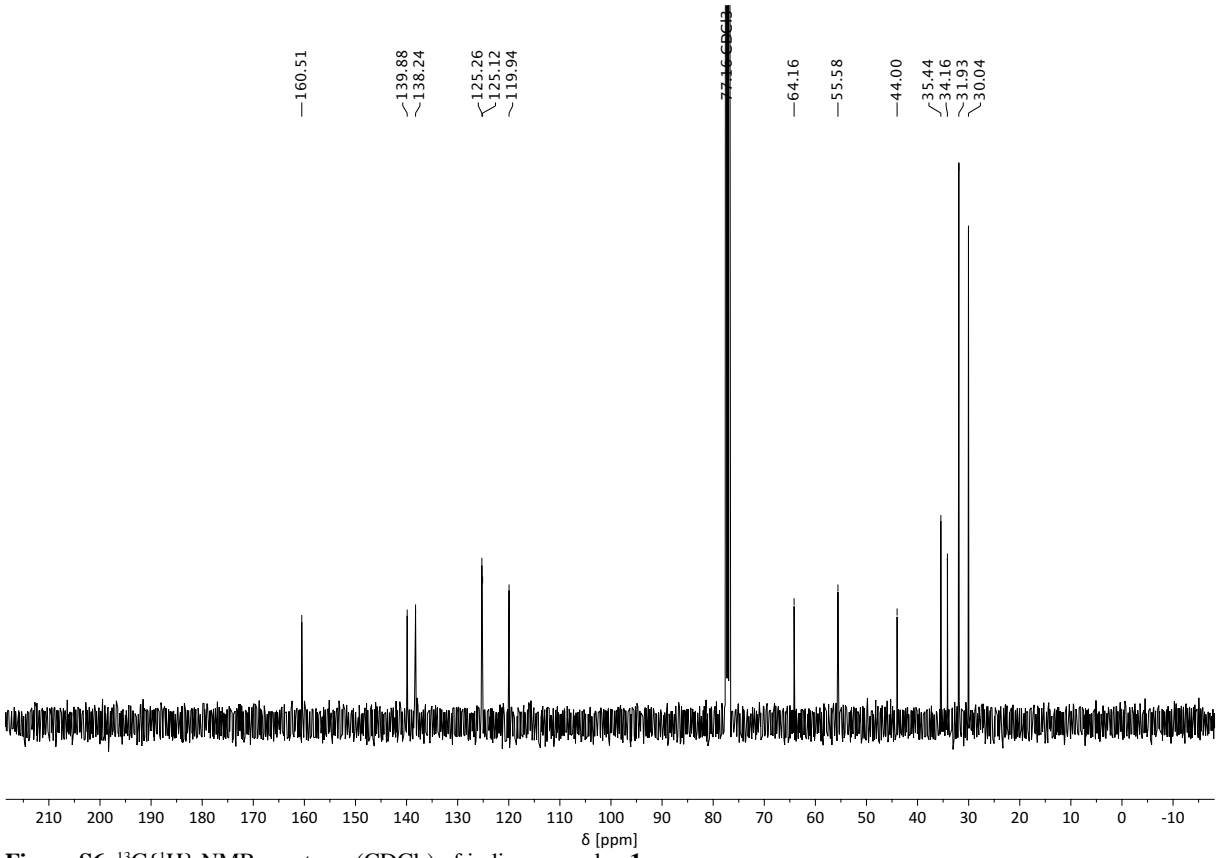

Figure S6. ^{13}C{^{1}H} NMR spectrum ($CDCl_3$) of indium complex **1**.

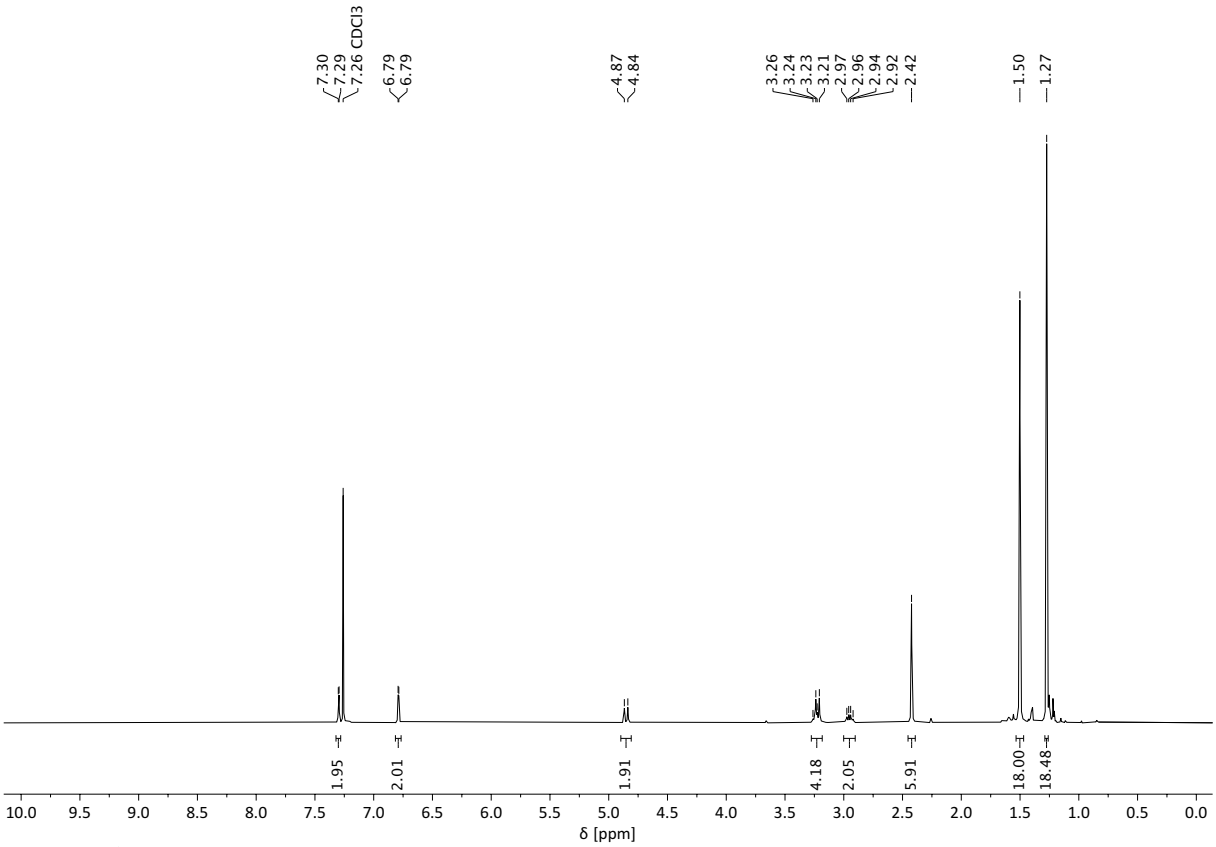

Figure S7. ^{1}H NMR spectrum ($CDCl_3$) of indium complex **1** stored under air at room temperature for 3 months.

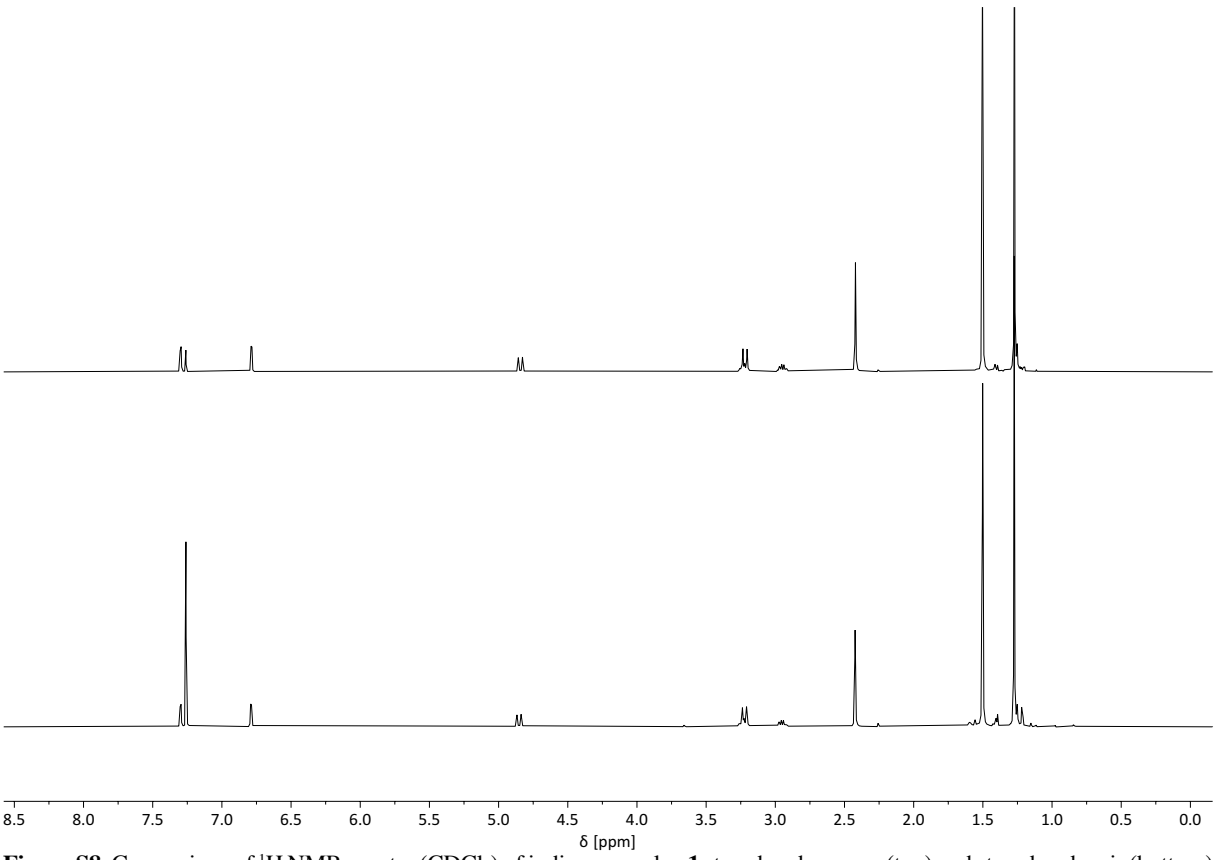

Figure S8. Comparison of ^{1}H NMR spectra ($CDCl_3$) of indium complex **1** stored under argon (top) and stored under air (bottom) at room temperature for 3 months.

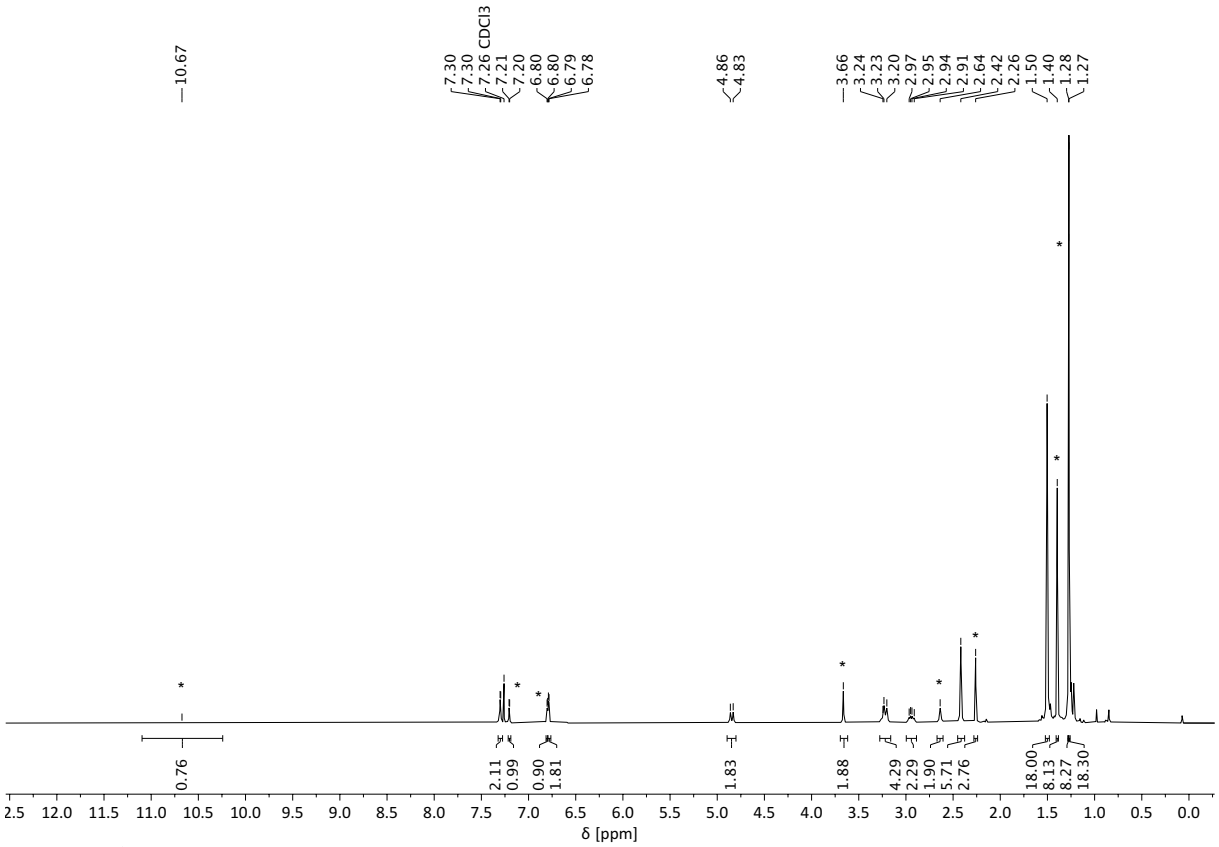

Figure S9. ^{1}H NMR spectrum ($CDCl_3$) of indium complex **1** after 20 h at room temperature in 0.5 ml hydrous $CDCl_3$ (water content: 110 ppm). Signals denoted with an asterisk belong to free salan ligand **L1**.

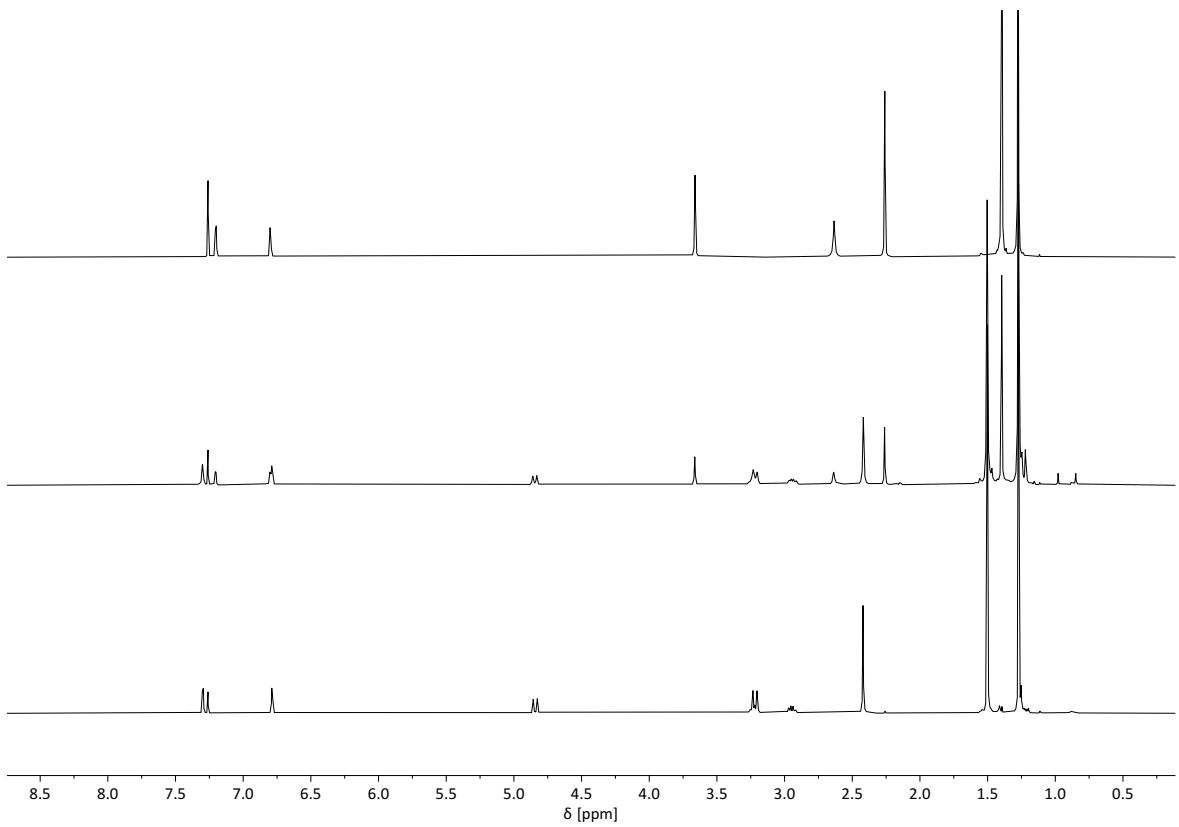

Figure S10. Comparison of ^{1}H NMR spectra ($CDCl_3$) of i) salan ligand **L1** (top), ii) indium complex **1** after 20 h at room temperature in 0.5 ml hydrous $CDCl_3$ (water content: 110 ppm) (middle), iii) indium complex **1** in dry $CDCl_3$ (bottom).

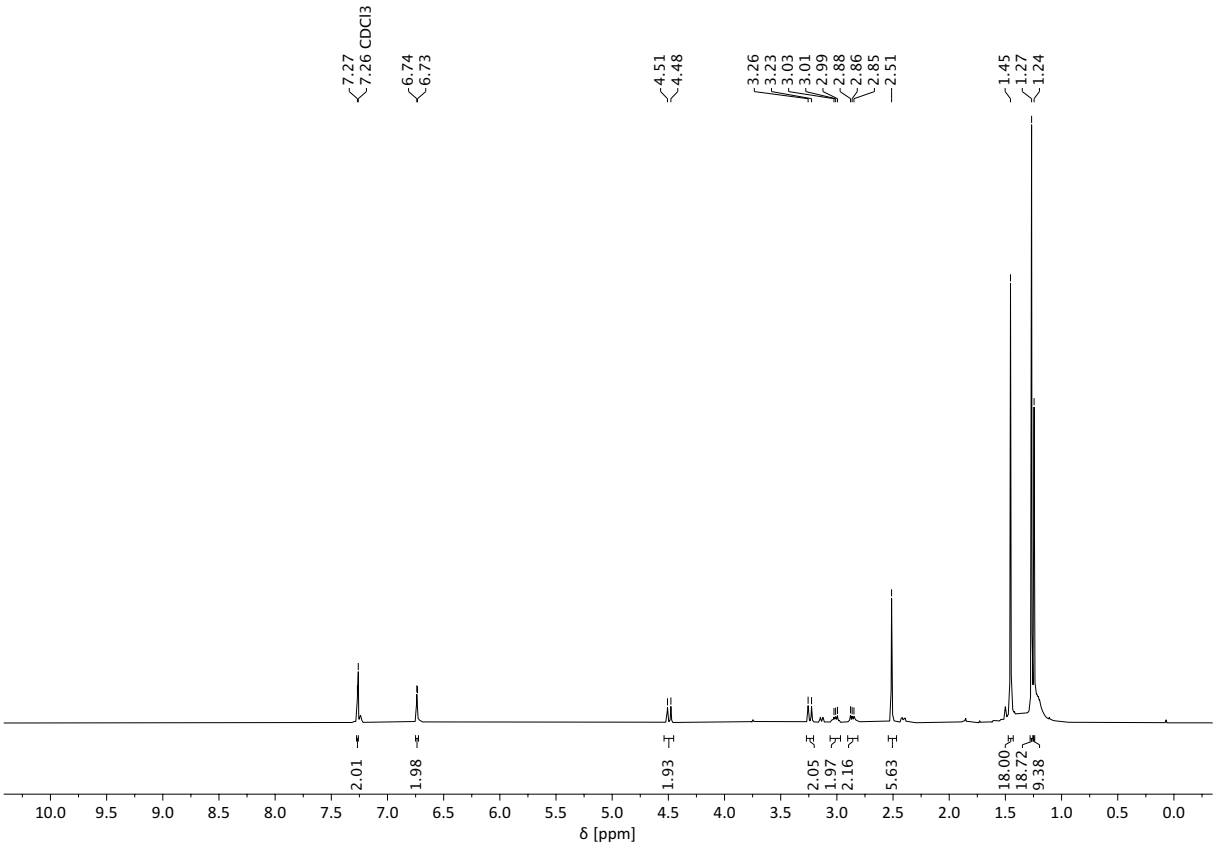

Figure S11. ^{1}H NMR spectrum ($CDCl_3$) of indium complex **2**.

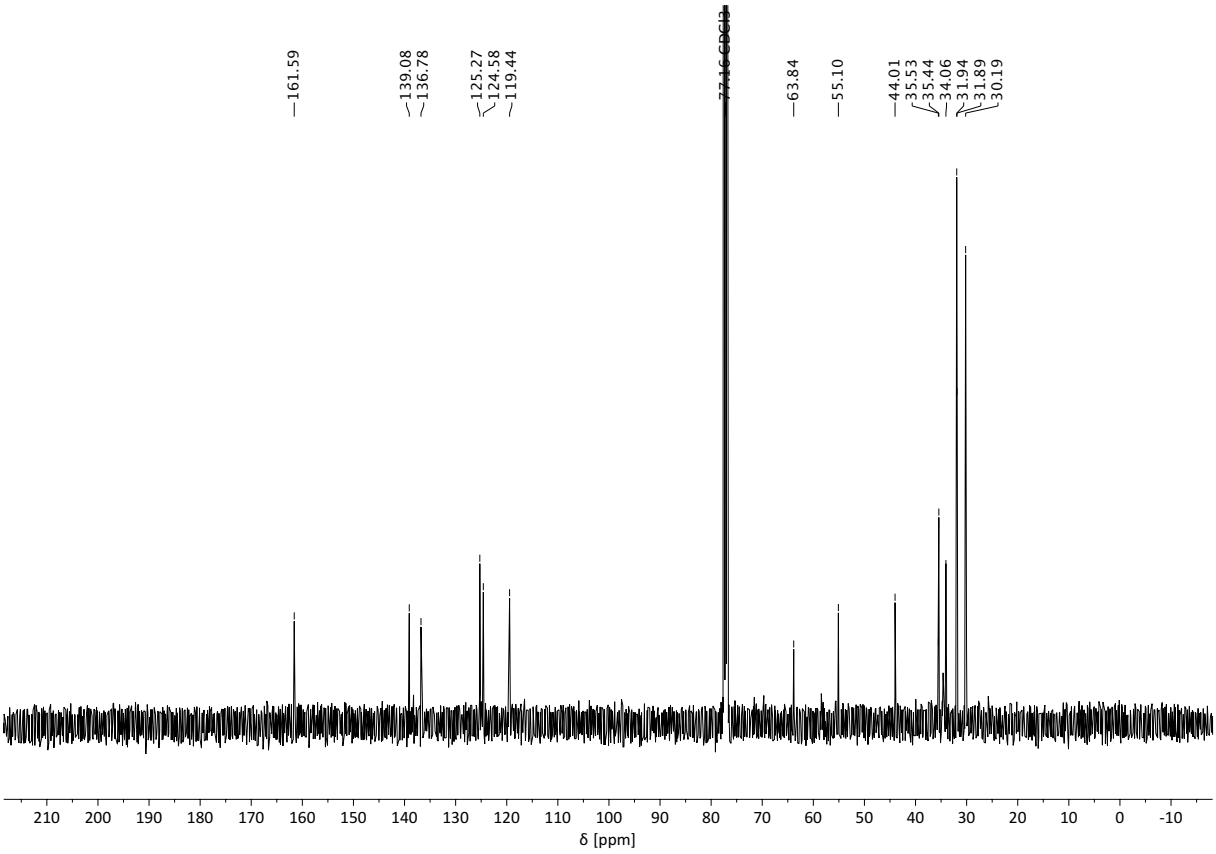

Figure S12. ^{13}C{^{1}H} NMR spectrum ($CDCl_3$) of indium complex **2**.

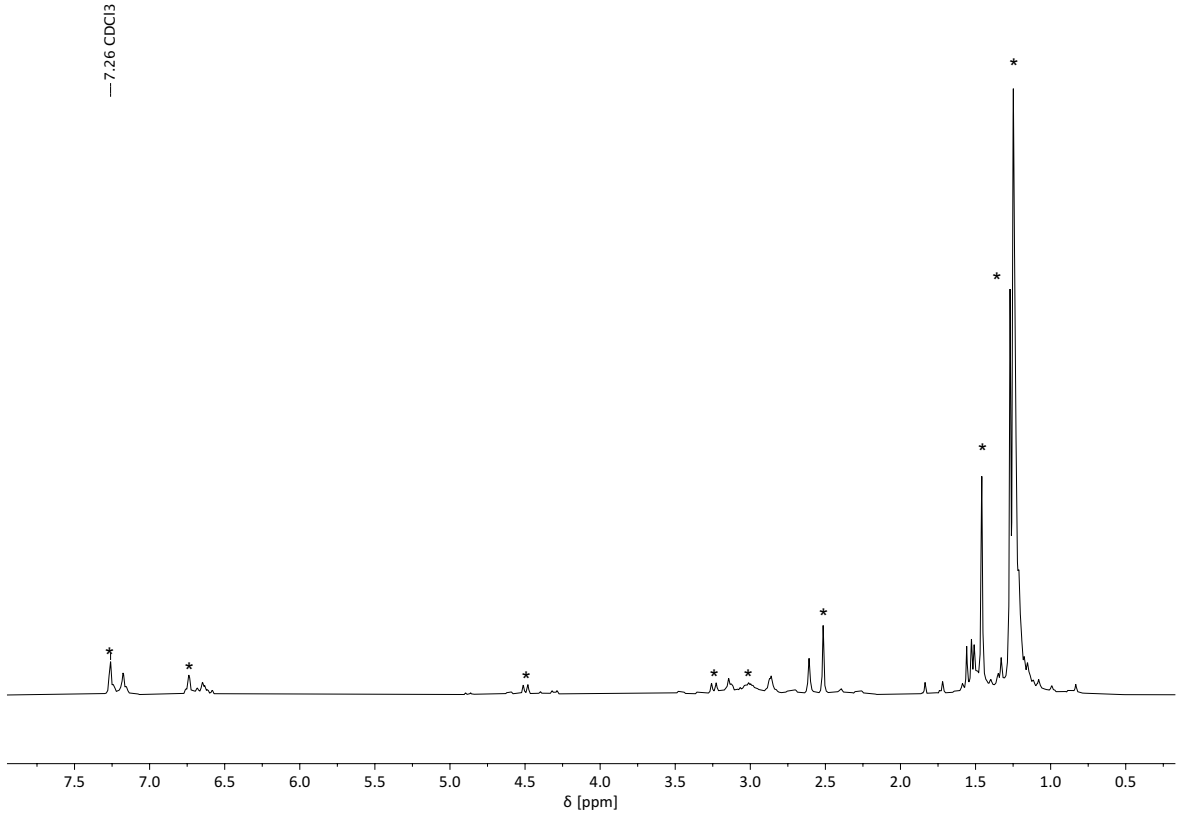

Figure S13. ^{1}H NMR spectrum ($CDCl_3$) of indium complex **2** stored under air at room temperature for 24 h. Signals denoted with an asterisk belong to complex **2**.

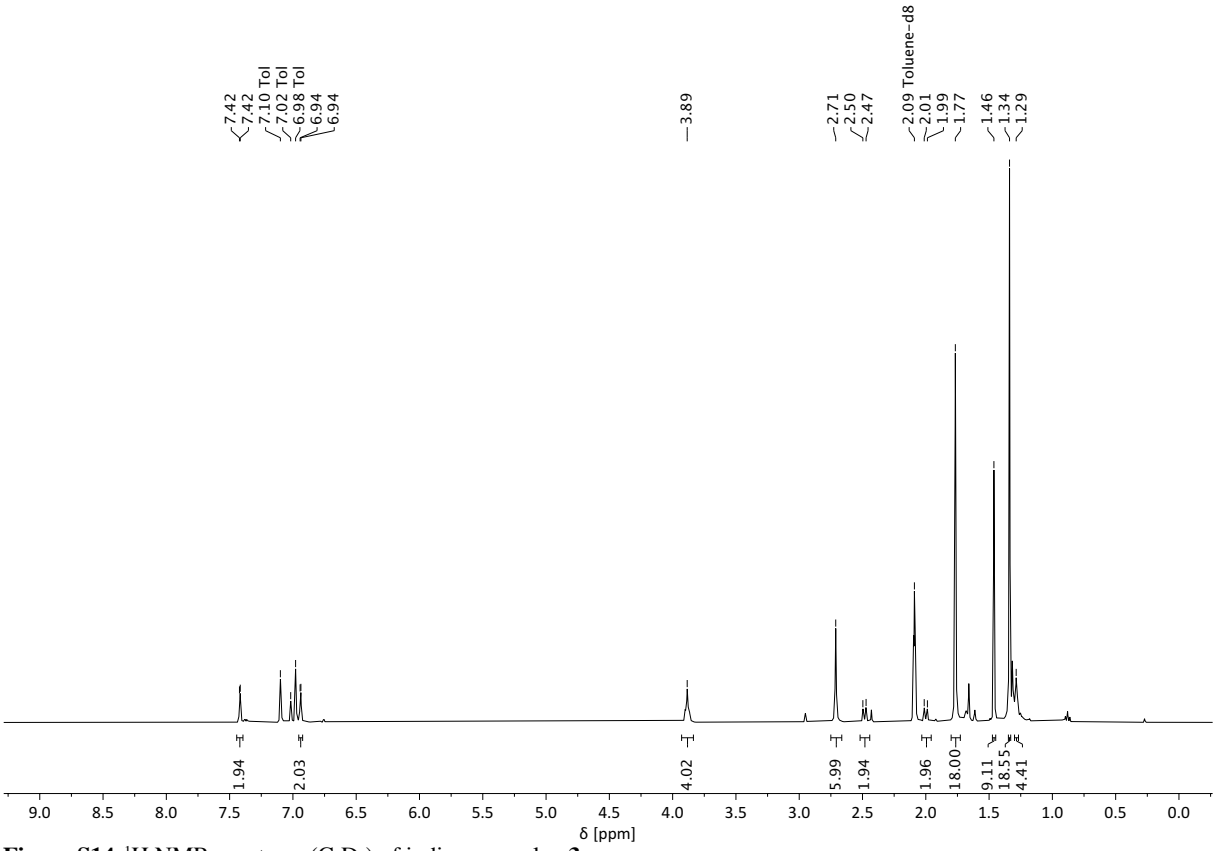

Figure S14. ^{1}H NMR spectrum (C_7D_8) of indium complex **3**.

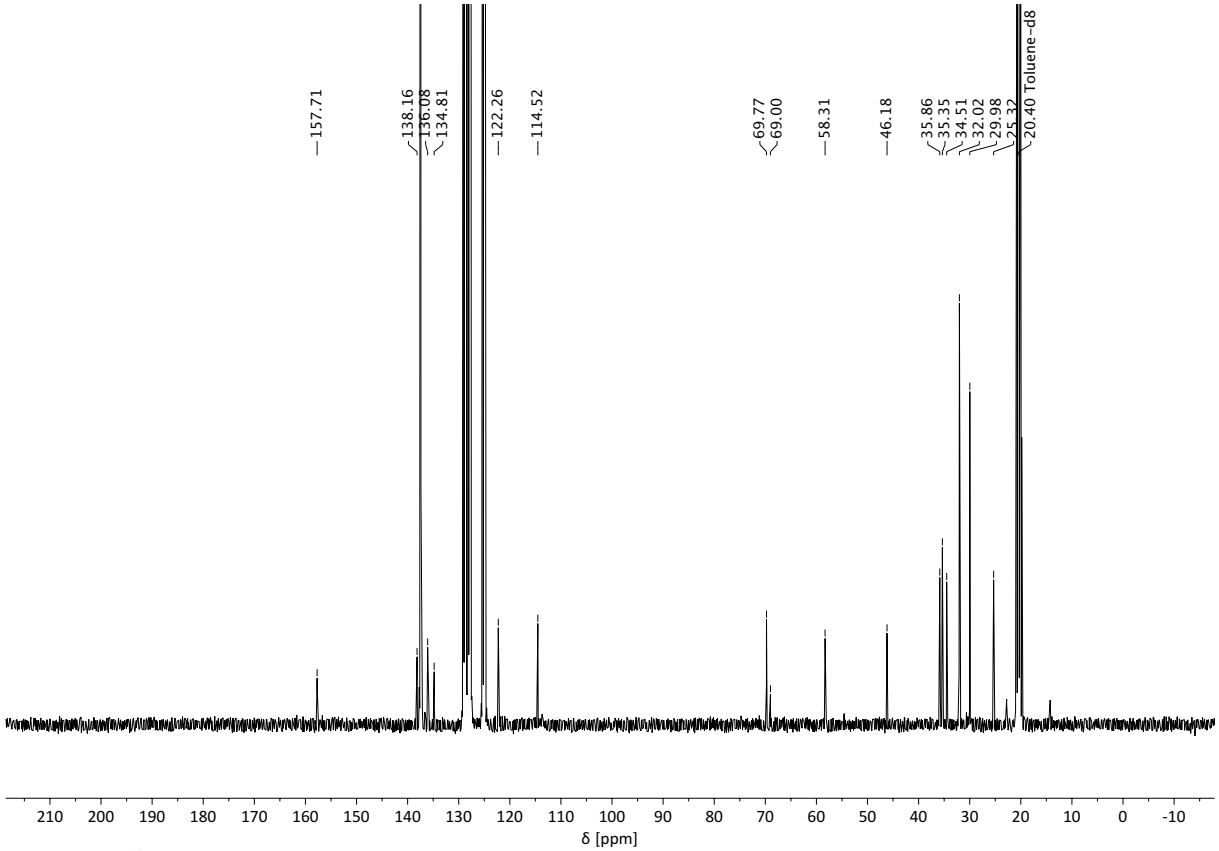

Figure S15. $^{13}C\{^{1}H\}$ NMR spectrum (C_7D_8) of indium complex **3**.

2. Polymerization Kinetics and Polymer Characterization Data

Table S1. Additional polymerization data [a]

entry	catalyst	monomer	[M]/[I]	time (min)	conv.[b] (%)	TOF (h^{-1})	M_n (theo.)[c] (kg mol^{-1})	M_n (GPC)[d] (kg mol^{-1})	$Đ$[d]
1	**1**	β-BL	200	1440	3	<1	n.d.	n.d.	n.d.
2[e]	**1**	β-BL	200	1440	63	5	10.8	32.5	1.39
3[f]	**1**	β-BL	200	60	0	0	n.d.	n.d.	n.d.
4[g]	**1**	β-BL	200	120	0	0	n.d.	n.d.	n.d.
5[h]	**2**	β-BL	200	30	97	388	16.7	26.7	1.07
6[i]	**2**	β-BL	200	30	73	292	12.6	18.5	1.05
7	**2**	β-BL	100	7	96	823	8.3	13.9	1.05
8	**2**	β-BL	150	10	96	864	12.4	19.9	1.04
9	**2**	β-BL	300	30	98	588	25.3	38.1	1.04
10	**2**	β-BL	400	15	82	1312	28.2	35.3	1.04
11	**2**	β-BL	800	60	60	480	41.3	56.5	1.05
12	**2**	β-BL	800	240	95	190	65.4	91.9	1.05

[a]Polymerizations were performed in toluene at room temperature, [β-BL] = 2.0 M. n.d. = not determined. [b]Conversion determined by ^{1}H NMR spectroscopy. [c]Theoretical molecular weights were determined from the [M]/[I] ratio and monomer conversion data. [d]Determined by GPC in $CHCl_3$ at room temperature relative to polystyrene standards. [e]T = 50°C. [f]Propylene oxide (PO) used as solvent. Preactivation time of catalyst in PO prior to monomer addition was 15 min. [g]10 equiv PO added. Preactivation time of catalyst prior to monomer addition was 24 h. [h]THF used as solvent. [i]CH_2Cl_2 used as solvent.

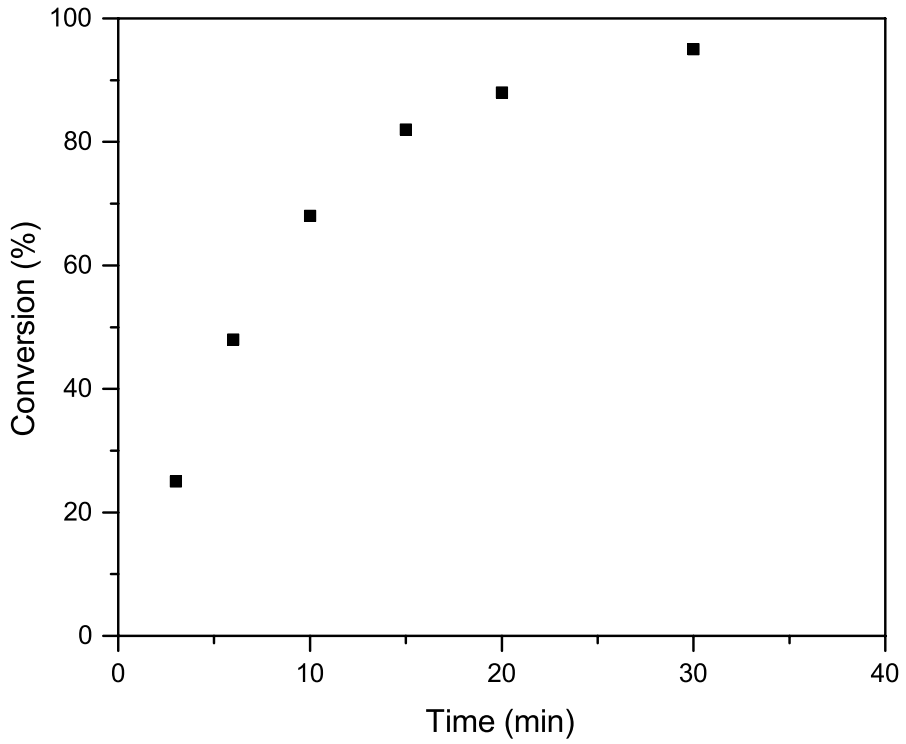

Figure S16. Conversion vs time plot for the ROP of β-BL using **2** as catalyst ([β-BL]/[**2**] = 400/1, T = rt., [β-BL] = 2.0 M).

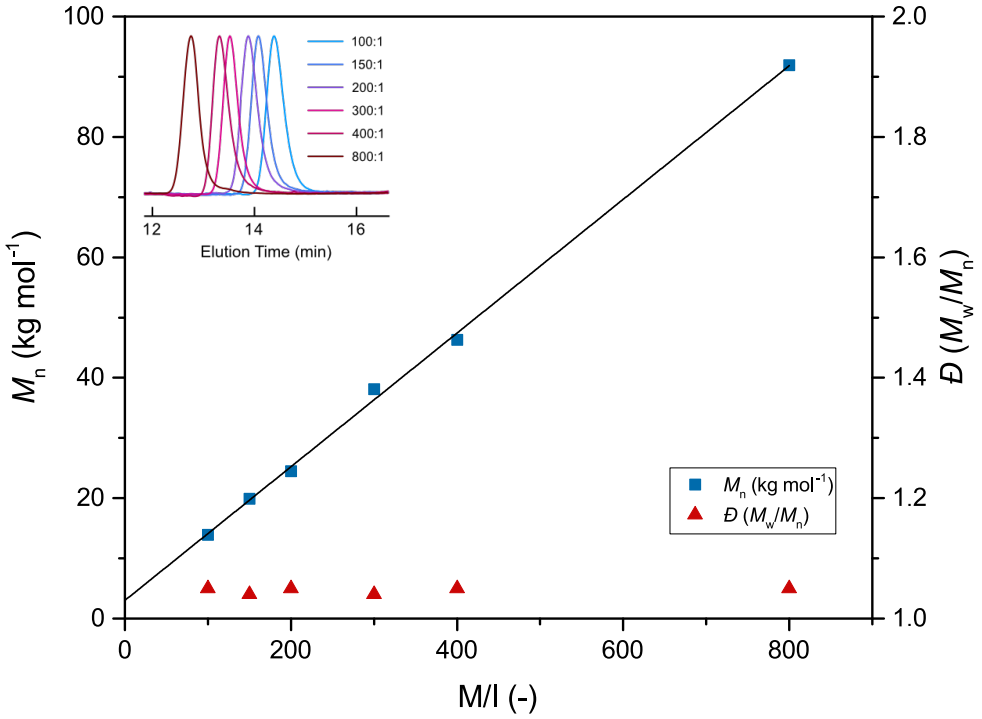

Figure S17. Plot of molecular weight and dispersity vs monomer-to-initiator ratio for the ROP of β-BL mediated by catalyst **2**. Inset: GPC traces of the polymers for different monomer-to-initiator ratios.

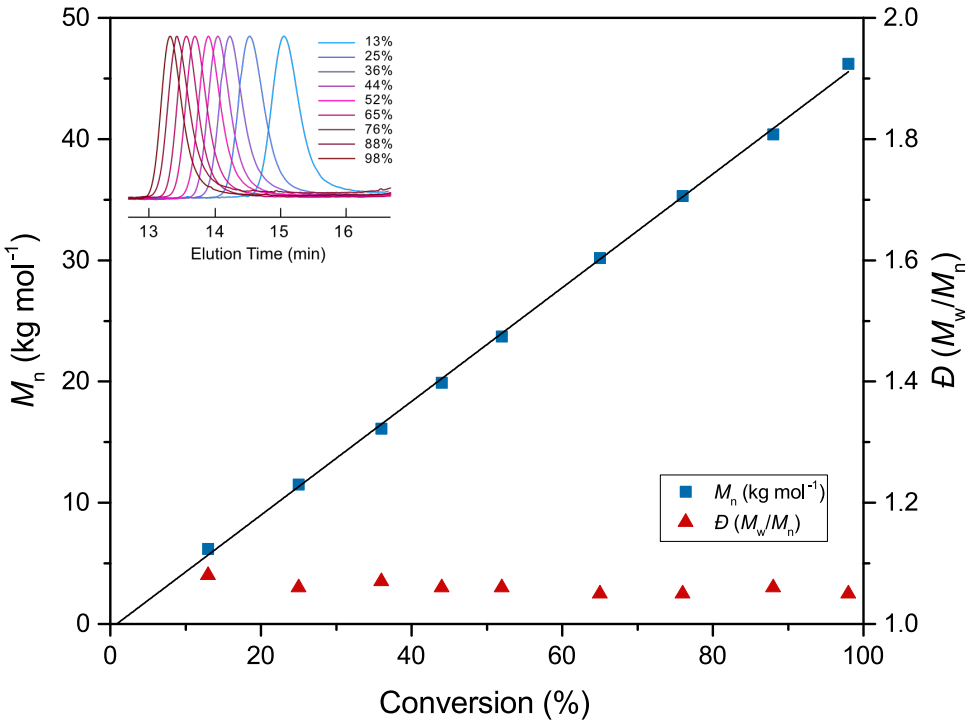

Figure S18. Evolution of molecular weight and dispersity with conversion for the ROP of β-BL mediated by catalyst **2**. Inset: GPC traces of the polymers at respective conversions.

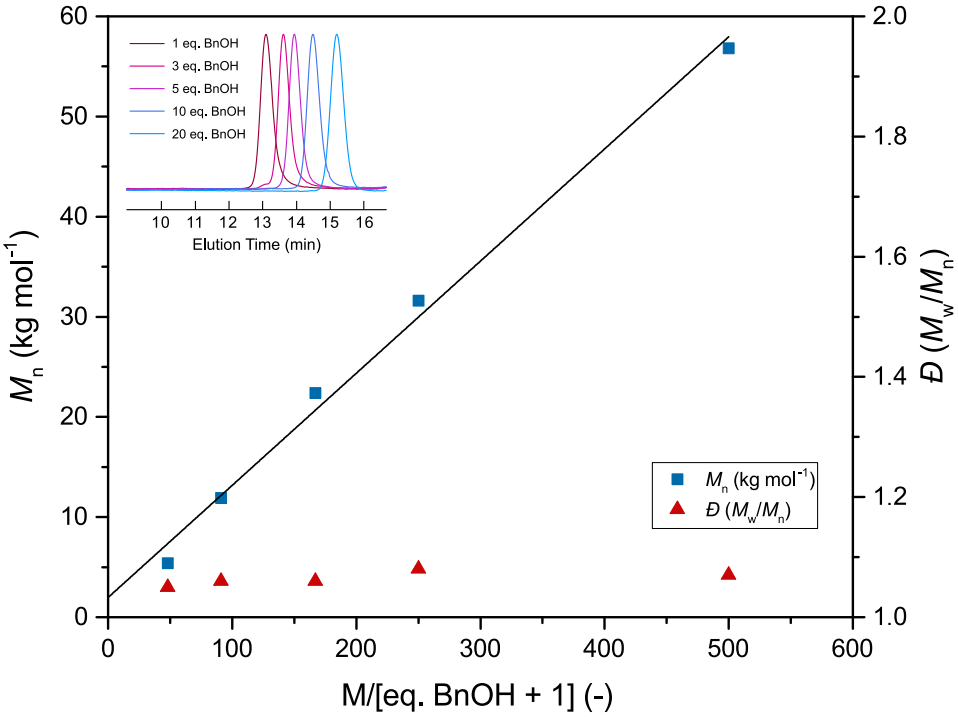

Figure S19. Immortal ROP of β-BL using catalyst **2** and BnOH as chain transfer agent. Plot of molecular weight and dispersity vs monomer-to-(BnOH + 1) ratio. Inset: GPC traces of the polymers with various amounts of chain transfer agent used in the ROP of β-BL.

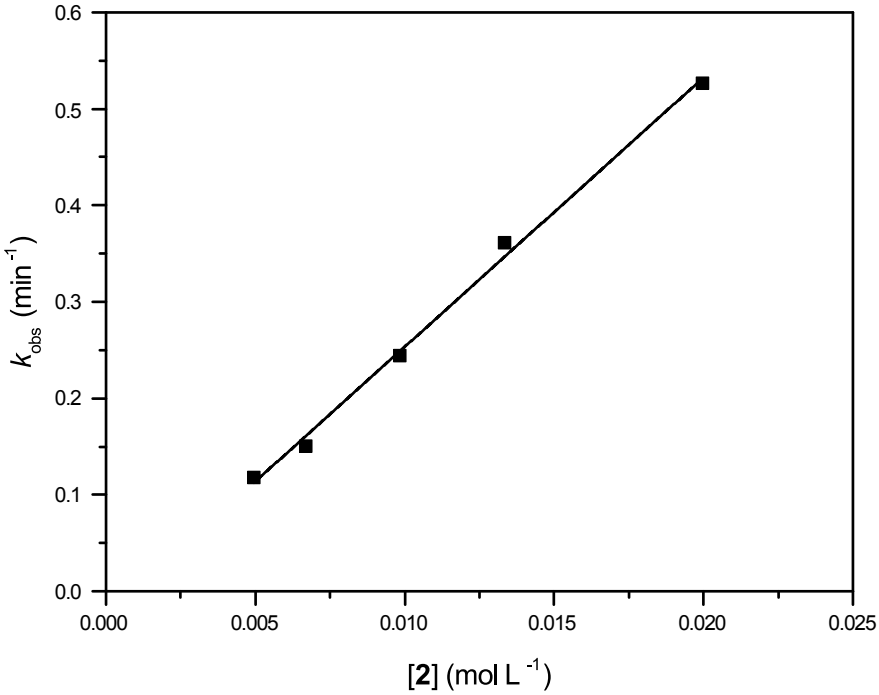

Figure S20. Plot of k_{obs} vs [**2**] for determination of propagation rate constant k_p. $k_p = 27.9 \pm 0.9$ L mol^{-1} min^{-1}, $R^2 = 0.997$.

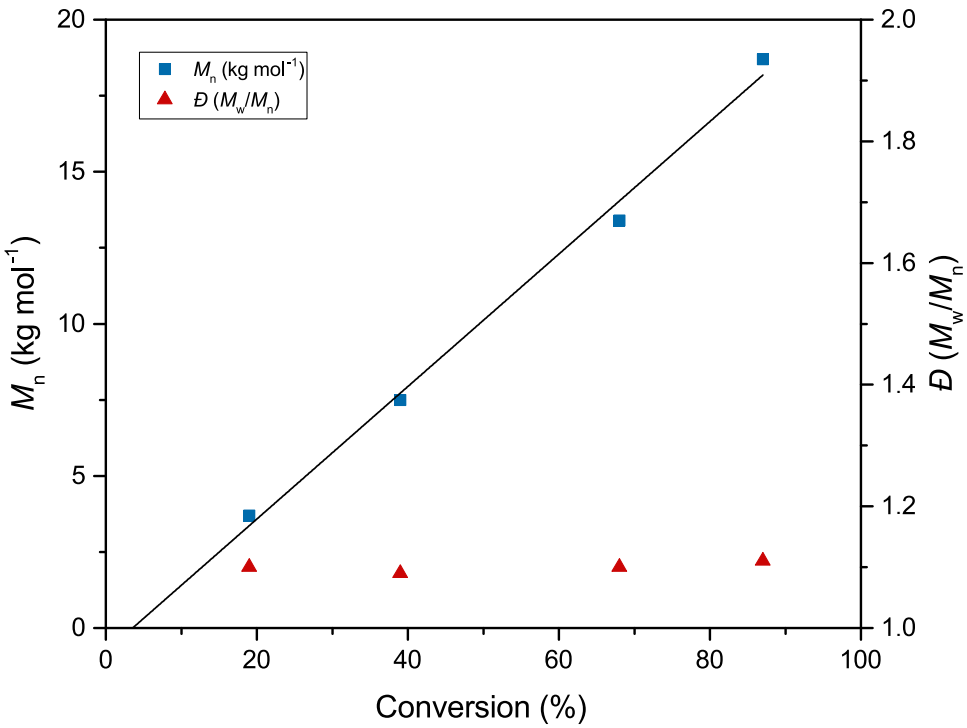

Figure S21. Evolution of molecular weight and dispersity with conversion for the ROP of β-BL mediated by complex **1** (activated for 24 h in PO prior to addition of β-BL).

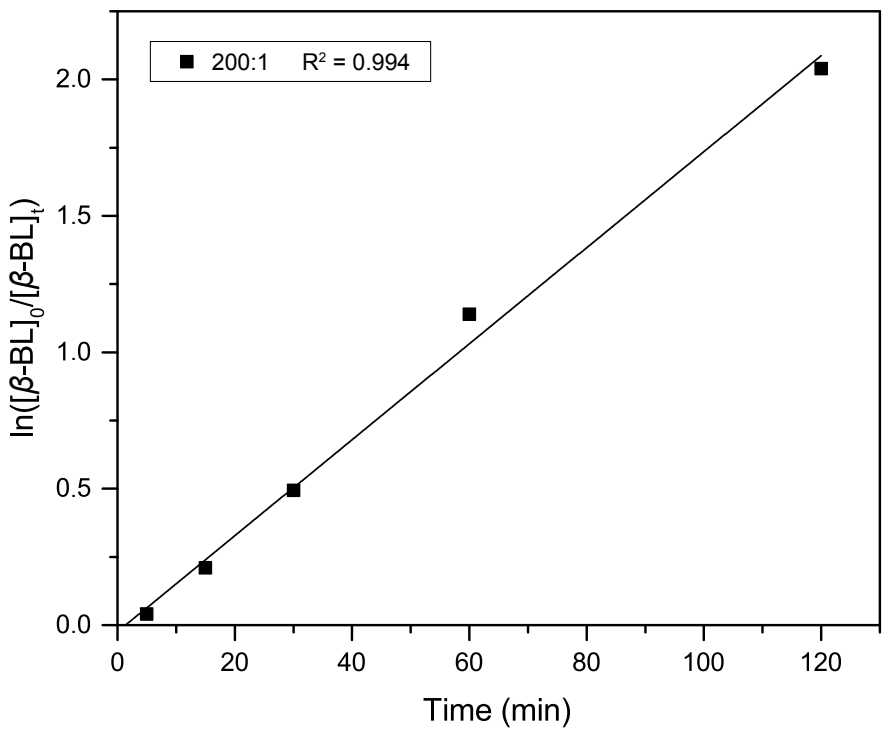

Figure S22. Semi-logarithmic plot of monomer concentration over time for the ROP of β-BL mediated by complex **1** (activated for 24 h in PO prior to addition of β-BL). k_{obs} = 0.018 ± 0.001 min^{-1}. Conditions: [β-BL]$_0$ = 2.0 M, [β-BL]/[**1**] = 200/1, T = rt.

Analysis of Polymer Microstructure

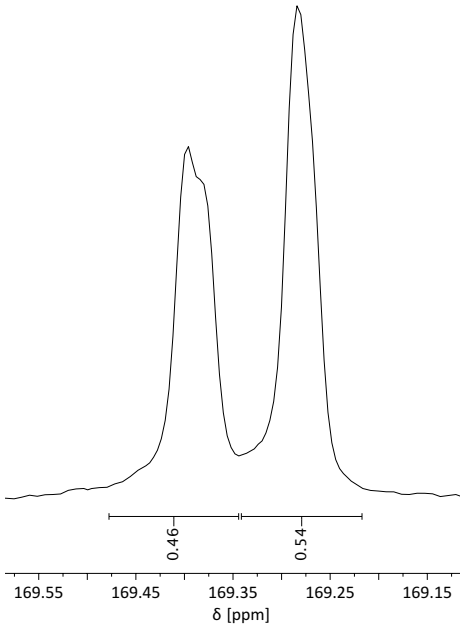

Figure S23. Representative $^{13}C\{^{1}H\}$ NMR spectrum (carbonyl region) of PHB produced by ROP of β-BL using **2** ($P_m = 0.54$).

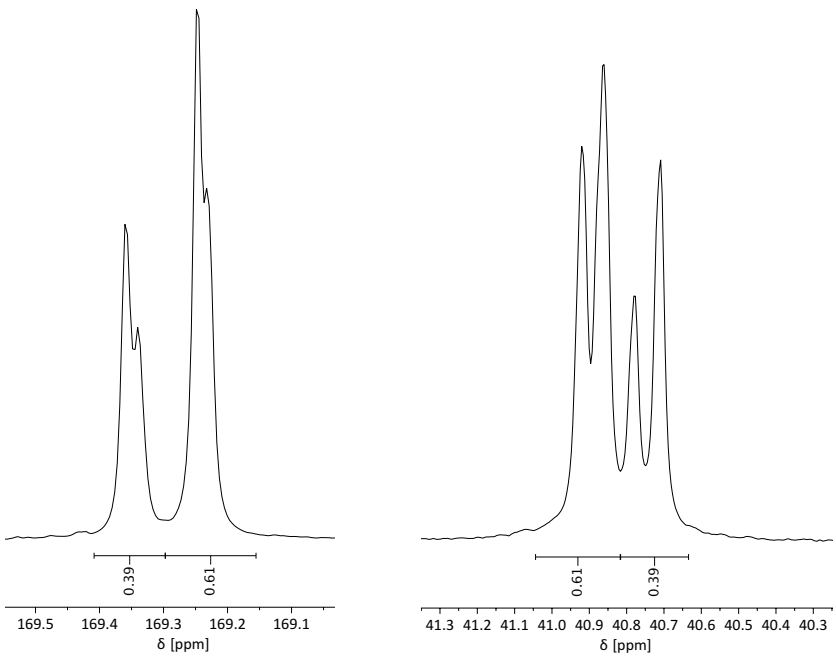

Figure S24. $^{13}C\{^{1}H\}$ NMR spectrum of PHB produced by ROP of β-BL using **3** ($P_m = 0.61$). Left: carbonyl region, right: methylene region.

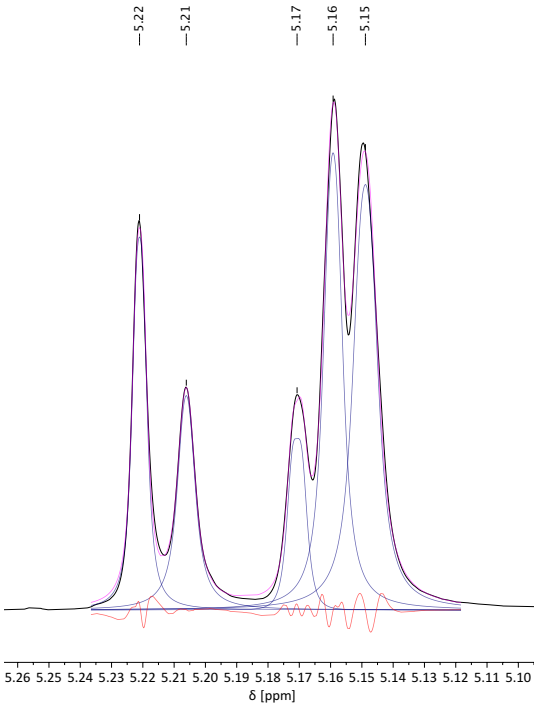

Figure S25. Representative peak deconvoluted $^{1}H\{^{1}H\}$ NMR spectrum (methine region) of PLA produced by ROP of *rac*-LA using **2** ($P_r = 0.62$).

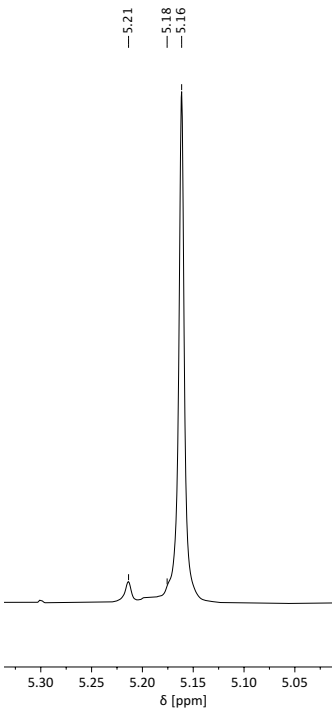

Figure S26. Peak deconvoluted $^{1}H\{^{1}H\}$ NMR spectrum (methine region) of PLA produced by ROP of unpurified *L*-LA using **2** ($P_m = 0.97$; Table 2, entry 11).

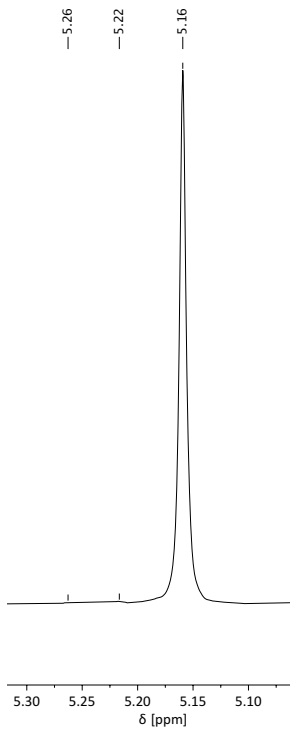

Figure S27. Peak deconvoluted $^{1}H\{^{1}H\}$ NMR spectrum (methine region) of PLA produced by ROP of unpurified *L*-LA using **2** ($P_m = 0.99$; Table 2, entry 12).

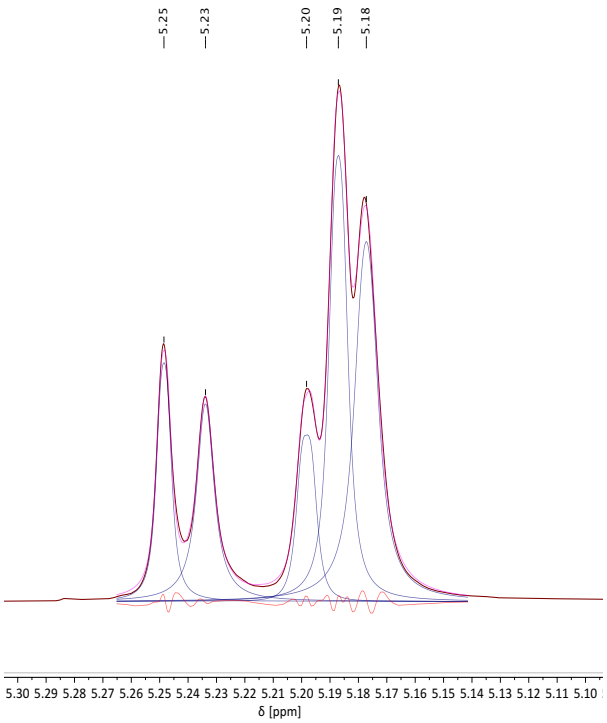

Figure S28. Peak deconvoluted $^{1}H\{^{1}H\}$ NMR spectrum (methine region) of PLA produced by ROP of *rac*-LA using **3** ($P_r = 0.57$).

Polymer End-Group Analysis

End-group analysis of oligomeric PHB produced by **2** ([β-BL]/[**2**] = 20/1) was carried out using ESI-MS and ^{1}H NMR measurements. The ESI-MS spectrum consisted of three series of molecular ion peaks with the major series (red squares) corresponding to linear PHB with ^{t}BuO/H chain ends and Na^+ (Figure S27). The respective series with K^+ was also observed (orange triangles). The third population corresponded to linear PHB with crotonyl chain ends (blue circles). Although the formation of crotonyl chain ends in ROP of β-BL is a well-known phenomenon, we consider that the side reaction is not caused by the catalyst during ROP but is in fact occurring during the ionization of the oligomeric sample in the ESI-MS measurements. This is also supported by end-group analysis using NMR spectroscopy (Figure S28). The identical sample of oligomeric PHB used for ESI-MS measurements showed no signals of crotonyl chain ends in the ^{1}H NMR spectrum but solely the corresponding methine proton (4.2 ppm) of linear PHB (Figure S28).

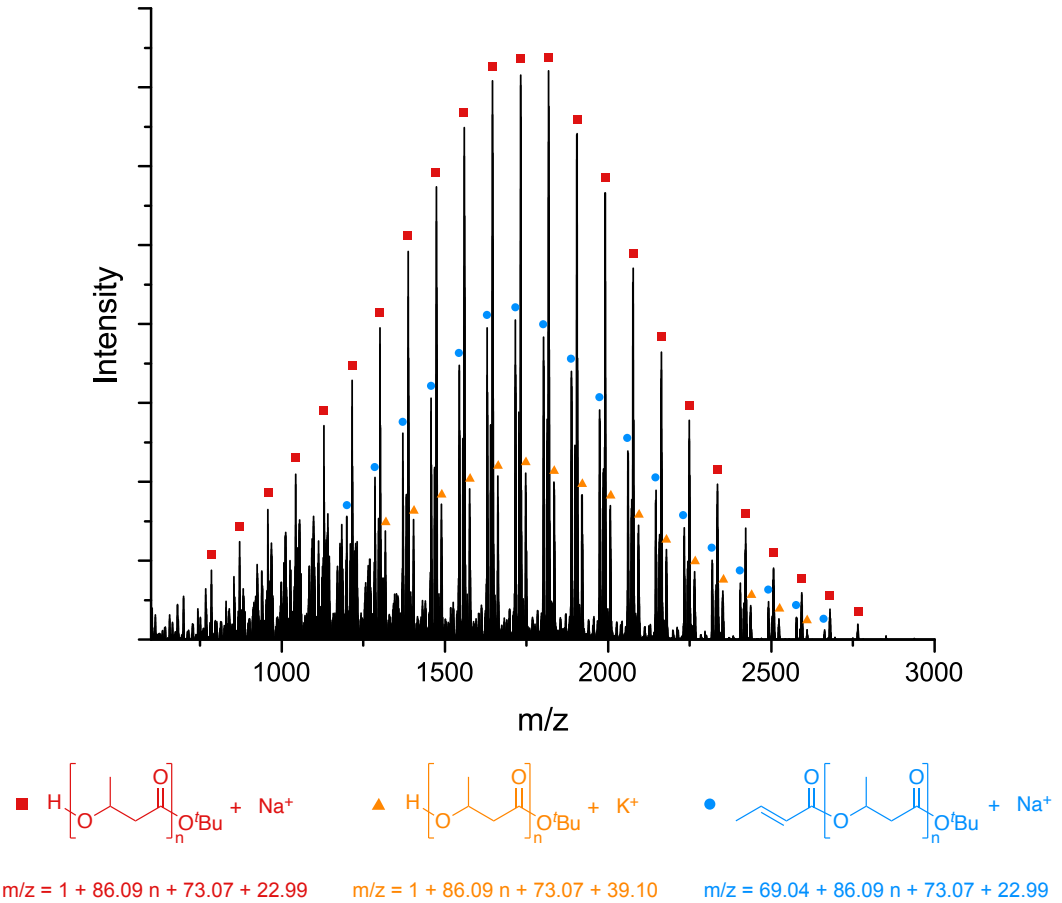

Figure S29. ESI-MS spectrum of PHB produced by **2** ([β-BL]/[**2**] = 20/1). For remarks on crotonyl chain ends see discussion above.

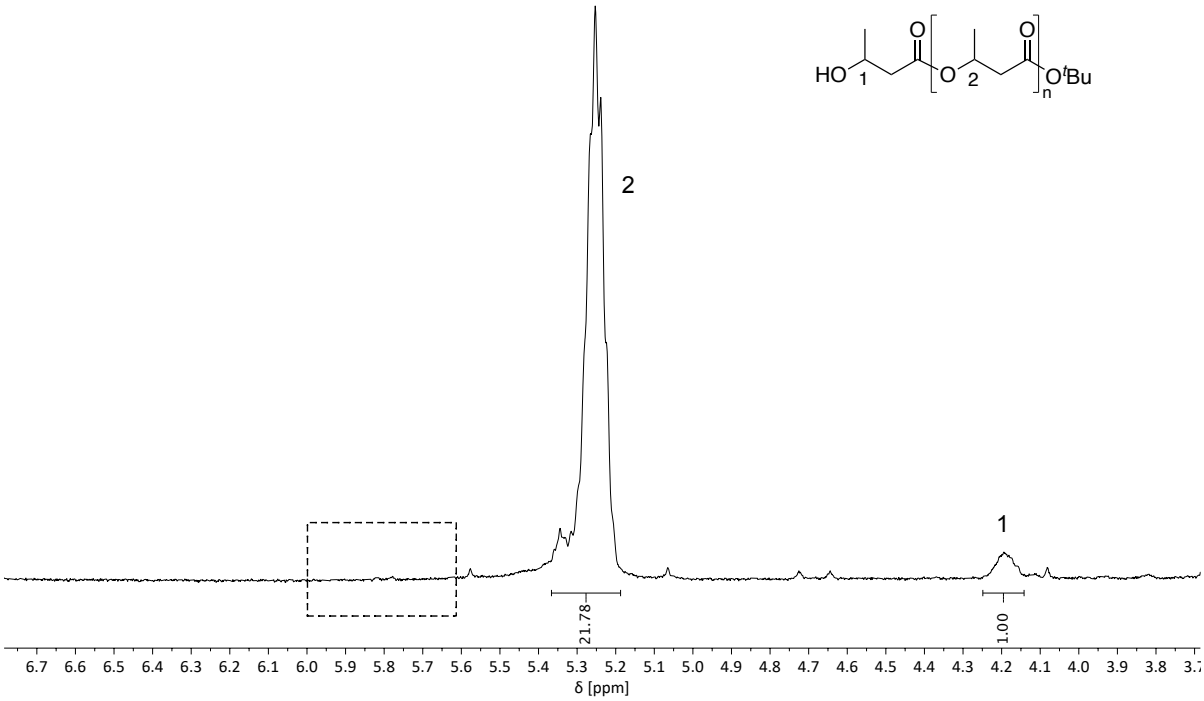

Figure S30. ^{1}H NMR spectrum ($CDCl_3$) of the methine region of PHB produced by **2** ([β-BL]/[**2**] = 20/1). The absence of signals corresponding to crotonyl chain ends is highlighted by the rectangle.

DOSY NMR Analysis of Compounds 2 and 3

DOSY NMR measurements were performed to elucidate the nuclearity of compounds **2** and **3** in solution under conditions relevant for polymerization runs. The molecular weight of the compounds was determined by using external calibration curves with normalized diffusion coefficients.[8] Toluene-d_8 was used as solvent and the diffusion coefficient of the residual solvent resonance used as an internal reference for calculations. An external calibration curve for dissipated spheres and ellipsoids was chosen (see ref. 8 for details). The observed diffusion coefficients of the analytes and the internal reference are given in Figures S29 and S30. A molecular weight of 450 g mol^{-1} and 642 g mol^{-1} was determined for compound **2** and **3**, respectively, indicating that both compounds are mononuclear in solution.

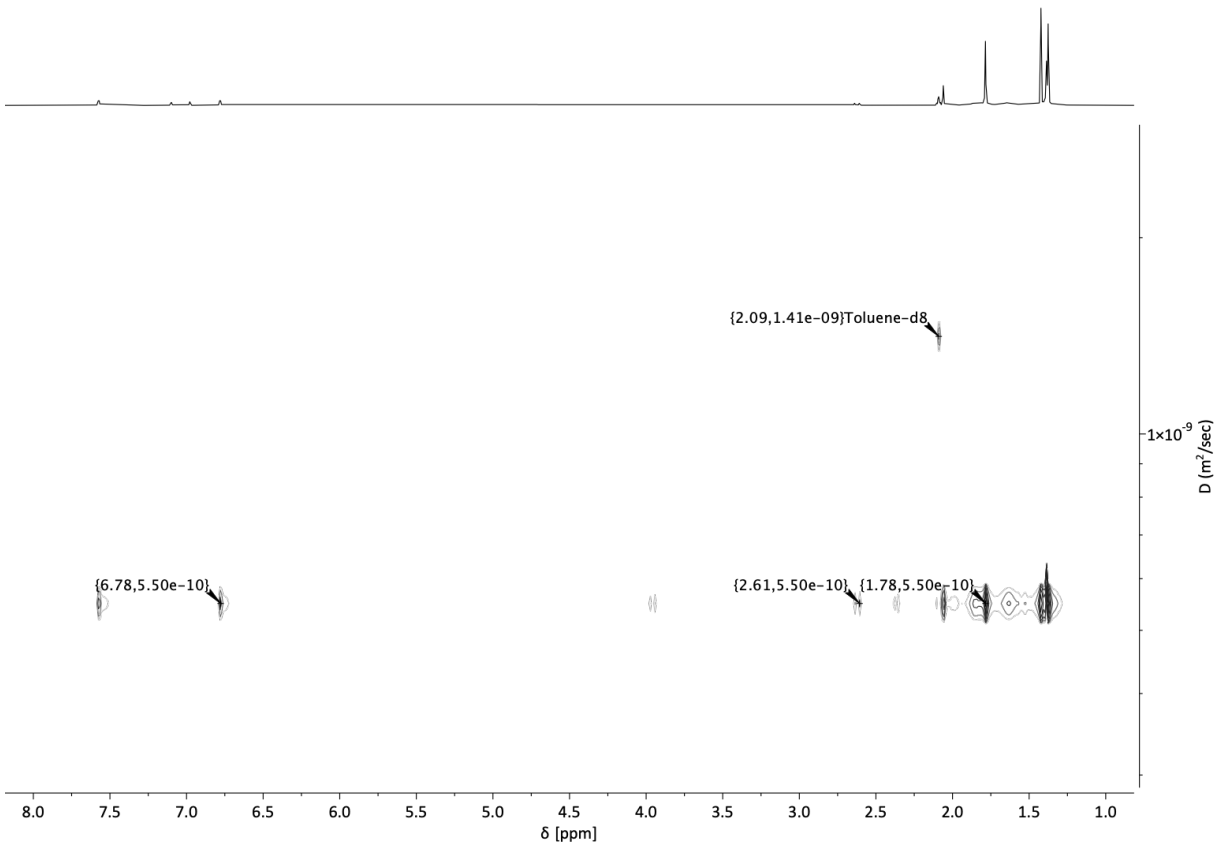

Figure S31. ^{1}H DOSY NMR of compound **2** in toluene-d_8 at room temperature.

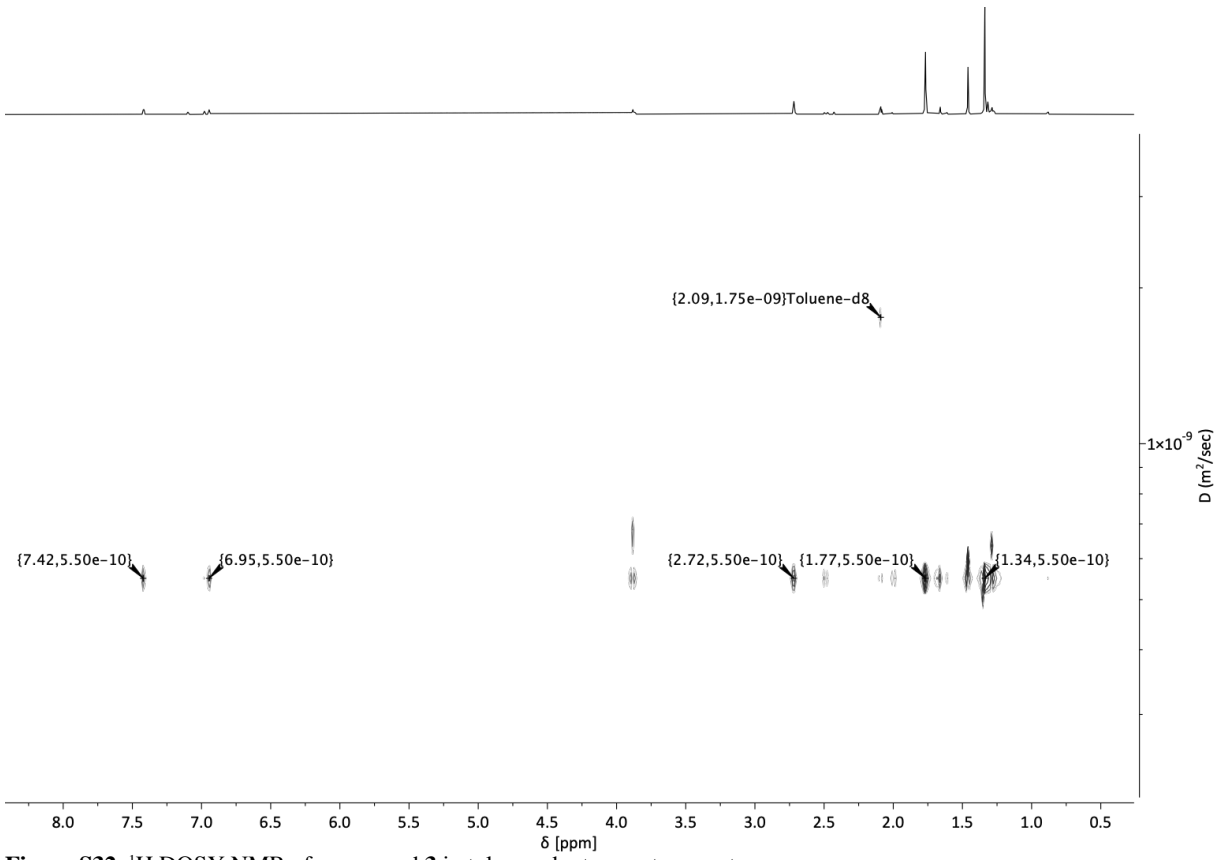

Figure S32. ^{1}H DOSY NMR of compound **3** in toluene-d_8 at room temperature.

Representative GPC Traces

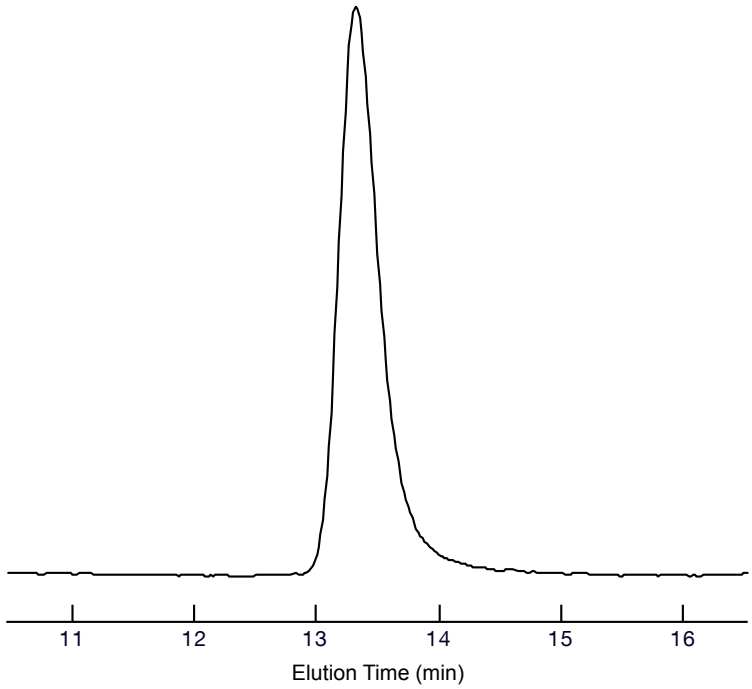

Figure S33. GPC trace of PHB by [β-BL]/[**2**] = 400/1 (M_n = 43.9 kg mol^{-1}, $Đ$ = 1.03).

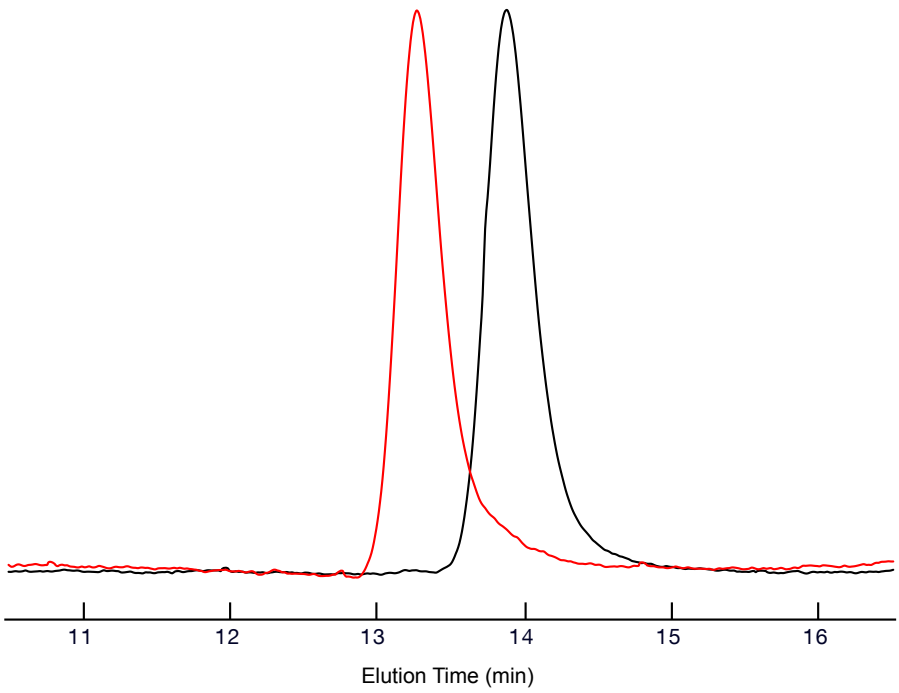

Figure S34. GPC traces of PHB of a chain extension experiment with catalyst **2**. Black: polymer after conversion of first 200 equiv of β-BL (M_n = 24.5 kg mol^{-1}, $Đ$ = 1.05). Red: polymer after conversion of second 200 equiv of β-BL (M_n = 48.0 kg mol^{-1}, $Đ$ = 1.06).

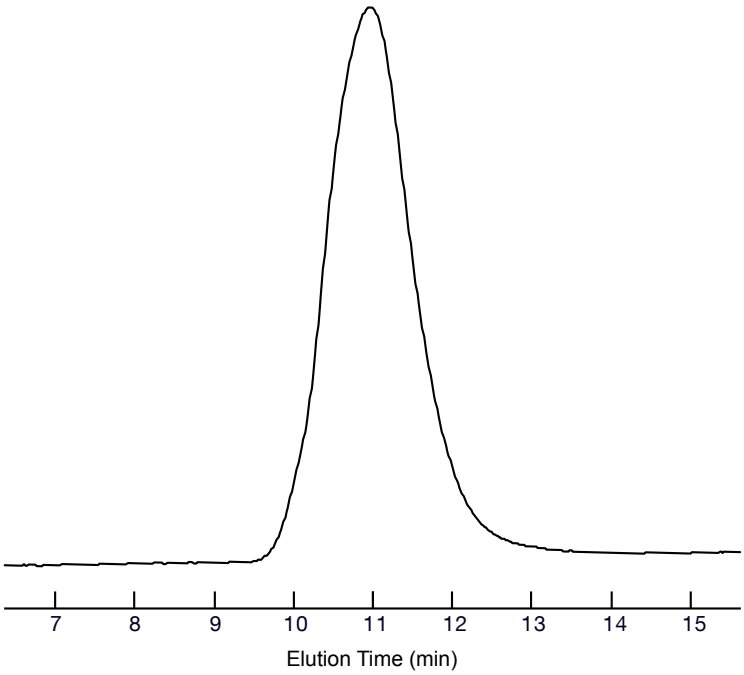

Figure S35. GPC trace of PεCL by [ε-CL]/[**2**] = 2000/1 ($M_{n,corr}$ = 318.8 kg mol^{-1}, $Đ$ = 1.49).

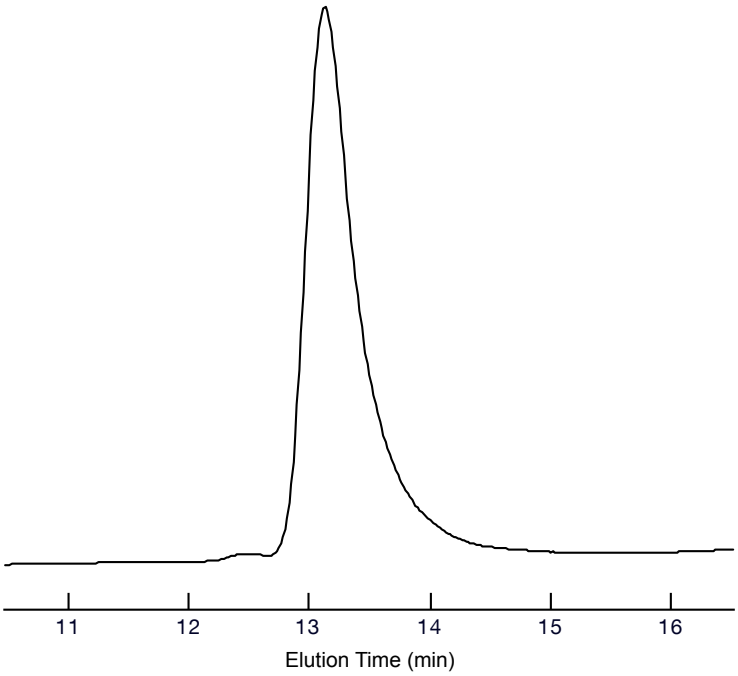

Figure S36. GPC trace of PεDL by [ε-DL]/[**2**] = 200/1 (M_n = 50.8 kg mol^{-1}, $Đ$ = 1.13).

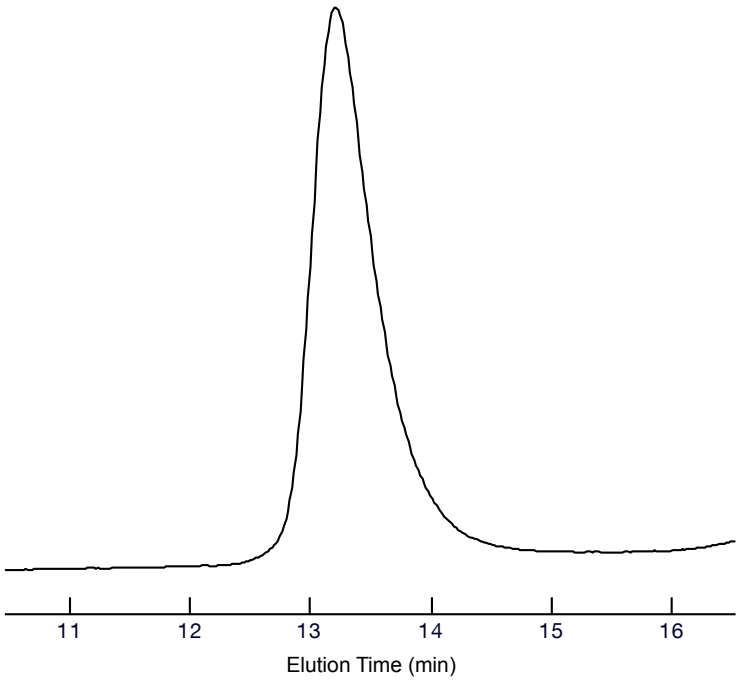

Figure S37. GPC trace of PLA by [*rac*-LA]/[**2**] = 500/1 ($M_{n,corr}$ = 26.8 kg mol^{-1}, $Đ$ = 1.15).

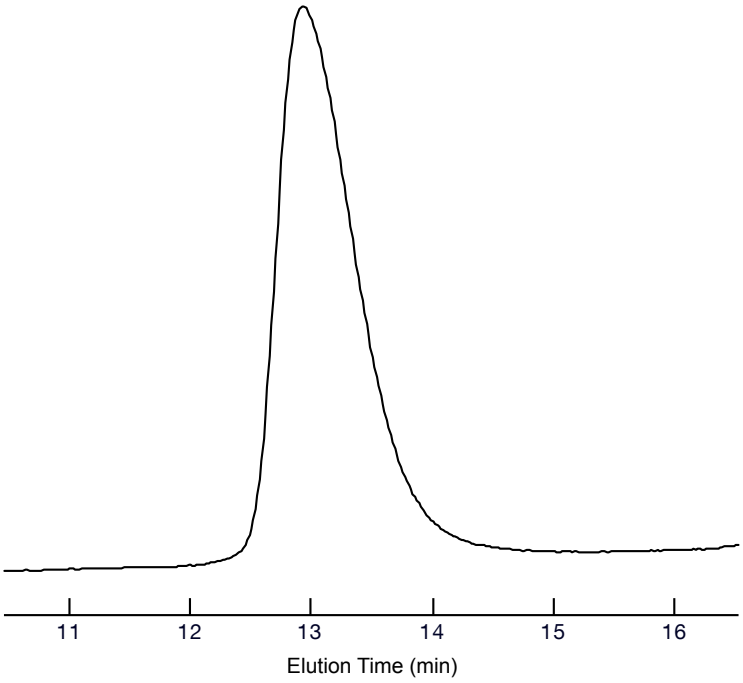

Figure S38. GPC trace of PLA by [*rac*-LA]/[**2**] = 1000/1, unpurified *rac*-LA used ($M_{n,corr}$ = 35.1 kg mol^{-1}, $Đ$ = 1.16).

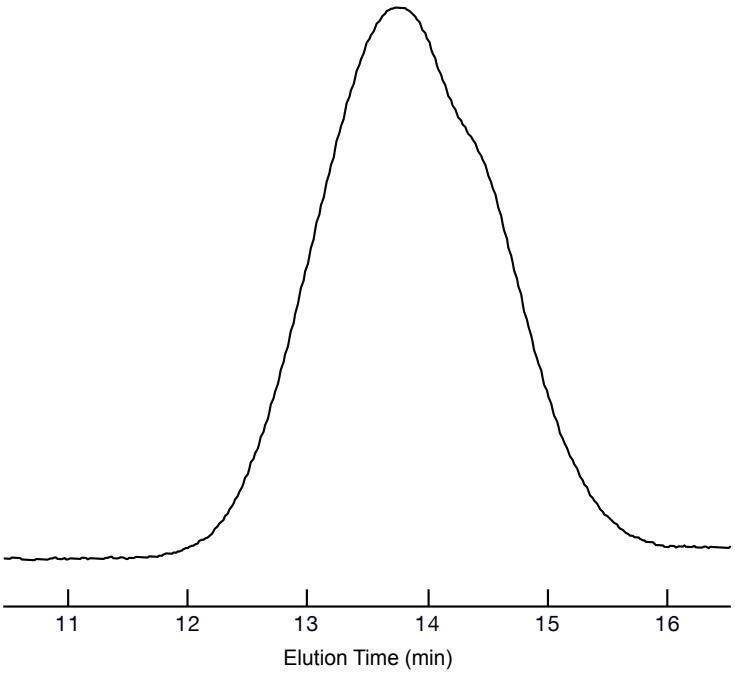

Figure S39. GPC trace of PγBL by [γ-BL]/[**2**] = 200/1 (M_n = 21.2 kg mol^{-1}, $Đ$ = 1.80).

3. X-Ray Crystallography

Single crystals of complex **2** were obtained by slow evaporation from a saturated toluene solution at room temperature and were measured following the details given below.

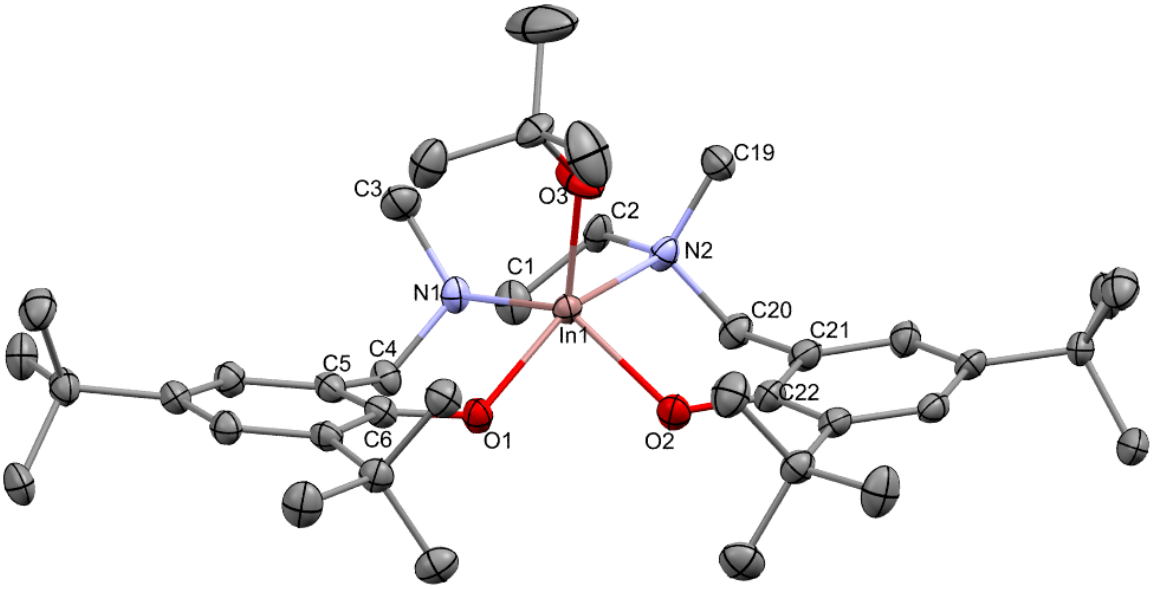

Figure S40. Molecular structure and numbering scheme of complex **2**: Displacement ellipsoids are drawn at the 50% probability level. Hydrogen atoms are omitted for clarity. Selected bond lengths and angles are given in Table S2.

General procedure

The X-ray data were collected on an X-ray single crystal diffractometer equipped with a CMOS detector (Bruker Photon-100), an IMS microsource with MoKα radiation (λ=0.71073Å) and a Helios mirror optic by using the APEX III software package.[9] The crystal was fixed on top of a microsampler using perfluorinated ether, transferred to the diffractometer and measured under a stream of cold nitrogen. A matrix scan was used to determine the initial lattice parameters. Reflections were corrected for Lorentz and polarization effects, scan speed, and background using SAINT.[10] Absorption corrections, including odd and even ordered spherical harmonics were performed using SADABS.[10] Space group assignments were based upon systematic absences, *E* statistics, and successful refinement of the structures. Structures were solved by SHELXT[11] (intrinsic phasing) with the aid of successive difference Fourier maps, and were refined against all data using with SHELXL2018[12] in conjunction with SHELXLE.[13] Methyl hydrogen atoms were refined as part of rigid rotating groups, with a C–H distance of 0.98 Å and Uiso(H)= 1.5·Ueq(C). Other H atoms were placed in calculated positions and refined using

a riding model, with methylene and aromatic C–H distances of 0.99 and 0.95Å, respectively, and Uiso(H)= 1.2·Ueq(C). Non-hydrogen atoms were refined with anisotropic displacement parameters. Full-matrix least-squares refinements were carried out by minimizing $\Delta w(Fo^2-Fc^2)^2$ with the SHELXL[12] weighting scheme. Neutral atom scattering factors for all atoms and anomalous dispersion corrections for the non-hydrogen atoms were taken from *International Tables for Crystallography*.[14] Images of the crystal structures were generated with MERCURY.[15] Crystallographic data are also deposited at the Cambridge Crystallographic Data Centre (CCDC 2128903) and are available free of charge via www.ccdc.cam.ac.uk/structures/.

Table S2. Selected bond lengths (Å) and angles (°) for the X-ray crystal structure of complex **2**.

Bond Length		**Bond Angle**		**Bond Angle**	
In1-O1	2.082(3)	O1-In1-N1	86.7(1)	O2-In1-N2	85.2(1)
In1-O2	2.065(4)	O1-In1-O2	83.5(1)	O2-In1-O3	120.3(1)
In1-O3	1.987(3)	O1-In1-N2	148.5(1)	N1-In1-N2	77.8(1)
In1-N1	2.304(3)	O1-In1-O3	121.9(1)	N1-In1-O3	107.2(1)
In1-N2	2.375(4)	O2-In1-N1	129.0(1)	N2-In1-O3	89.1(1)

Table S3. Crystallographic data for complex **2** (CCDC 2128903).

Diffractometer operator: Daniel Henschel
scanspeed 9 s per frame
dx 30 mm
2287 frames measured in 15 data sets
phi-scans with delta_phi = 0.5
omega-scans with delta_omega = 0.5
shutterless mode

Crystal data

$C_{38}H_{63}InN_2O_3$	$F(000)$ = 754
M_r = 710.72	
Triclinic, *P*	D_x = 1.239 Mg m^{-3}
Hall symbol: -P 1	Melting point: ? K
a = 11.4082 (16) Å	Mo $K\alpha$ radiation, λ = 0.71073 Å
b = 13.035 (2) Å	Cell parameters from 9943 reflections
c = 14.939 (2) Å	θ = 2.3–25.4°
α = 66.497 (6)°	μ = 0.66 mm^{-1}
β = 68.941 (6)°	T = 100 K
γ = 83.213 (7)°	Clear fragment, colourless

V = 1900.3 (5) Å^3	0.32 × 0.30 × 0.12 mm
Z = 2	

Data collection

Bruker Photon CMOS diffractometer	6944 independent reflections
Radiation source: IMS microsource	6024 reflections with $I > 2\sigma(I)$
Helios optic monochromator	R_{int} = 0.072
Detector resolution: 16 pixels mm^{-1}	θ_{max} = 25.4°, θ_{min} = 1.8°
phi– and ω–rotation scans	h = –13 13
Absorption correction: multi-scan *SADABS* 2016/2, Bruker, 2016	k = –15 15
T_{min} = 0.634, T_{max} = 0.745	l = –17 17
53587 measured reflections	

Refinement

Refinement on F^2	Secondary atom site location: difference Fourier map
Least-squares matrix: full	Hydrogen site location: inferred from neighbouring sites
$R[F^2 > 2\sigma(F^2)]$ = 0.042	H-atom parameters constrained
$wR(F^2)$ = 0.105	W = 1/[$\Sigma^2(FO^2)$ + (0.0454P)^2 + 5.4852P] WHERE P = (FO^2 + 2FC^2)/3
S = 1.00	$(\Delta/\sigma)_{max}$ < 0.001
6944 reflections	$\Delta\rho_{max}$ = 0.87 e Å^{-3}
414 parameters	$\Delta\rho_{min}$ = –0.85 e Å^{-3}
0 restraints	Extinction correction: none
? constraints	Extinction coefficient: ?
Primary atom site location: iterative	

4. References

1. Min, K. S.; Weyhermüller, T.; Bothe, E.; Wieghardt, K., Tetradentate Bis(*o*-iminobenzosemiquinonate(1−)) π Radical Ligands and Their *o*-Aminophenolate(1−) Derivatives in Complexes of Nickel(II), Palladium(II), and Copper(II). *Inorg. Chem.* **2004,** *43*, 2922-2931.

2. Bloembergen, S.; Holden, D. A.; Bluhm, T. L.; Hamer, G. K.; Marchessault, R. H., Stereoregularity in synthetic *β*-hydroxybutyrate and *β*-hydroxyvalerate homopolyesters. *Macromolecules* **1989,** *22*, 1656-1663.

3. Aluthge, D. C.; Ahn, J. M.; Mehrkhodavandi, P., Overcoming aggregation in indium salen catalysts for isoselective lactide polymerization. *Chem. Sci.* **2015,** *6*, 5284-5292.

4. Save, M.; Schappacher, M.; Soum, A., Controlled ring-opening polymerization of lactones and lactides initiated by lanthanum isopropoxide, 1. General aspects and kinetics. *Macromol. Chem. Phys.* **2002,** *203*, 889-899.

5. Schneider, F.; Zhao, T.; Huhn, T., Cytotoxic heteroleptic heptacoordinate salan zirconium(iv)-bis-chelates - synthesis, aqueous stability and X-ray structure analysis. *Chem. Commun.* **2016,** *52*, 10151-10154.

6. Meppelder, G.-J. M.; Fan, H.-T.; Spaniol, T. P.; Okuda, J., Group 4 Metal Complexes Supported by [ONNO]-Type Bis(*o*-aminophenolato) Ligands: Synthesis, Structure, and α-Olefin Polymerization Activity. *Organometallics* **2009,** *28*, 5159-5165.

7. Beament, J.; Mahon, M. F.; Buchard, A.; Jones, M. D., Salan group 13 complexes – structural study and lactide polymerisation. *New J. Chem.* **2017,** *41*, 2198-2203.

8. Neufeld, R.; Stalke, D., Accurate molecular weight determination of small molecules *via* DOSY-NMR by using external calibration curves with normalized diffusion coefficients. *Chem. Sci.* **2015**, *6*, 3354-3364.

9. APEX suite of crystallographic software, APEX 3, version 2019.1-0, Bruker AXS Inc.: Madison, Wisconsin, USA, **2019**.

10. SAINT, Version 8.40a and SADABS Version 2016/2, Bruker AXS Inc.: Madison, Wisconsin, USA **2017**.

11. Sheldrick, G. M. SHELXT-2014/5, University of Göttingen: Göttingen, Germany, **2014**.

12. Sheldrick, G. M. SHELXL-2018/3, University of Göttingen: Göttingen, Germany, **2018**.

13. Huebschle, C. B.; Sheldrick, G. M.; Dittrich, B., SHELXLE. *J. Appl. Cryst.* **2011**, *44*, 1281.

14. Wilson, A. J. C., *International Tables for Crystallography, Vol. C.* Kluwer Academic Publishers: Dordrecht, Netherlands **1992**.

15. C. F. Macrae, I. Sovago, S. J. Cottrell, P. T. A. Galek, P. McCabe, E. Pidcock, M. Platings, G. P. Shields, J. S. Stevens, M. Towler and P. A. Wood, Mercury 4.0: from visualization to analysis, design and prediction. *J. Appl. Cryst.* **2020**, *53*, 226-235.